AD-A146 545 MILLIMETER-WAVE TRAVELLING-WAVE IMPATT DIODE(U) TEXAS UNIV AT AUSTIN MICROWAVE LAB Y FUKUOKA ET AL. 31 MAY 84 NW-84-7 ARO-17735.35-EL DAAG29-81-K-0053 1/1

UNCLASSIFIED F/G 9/1 NL

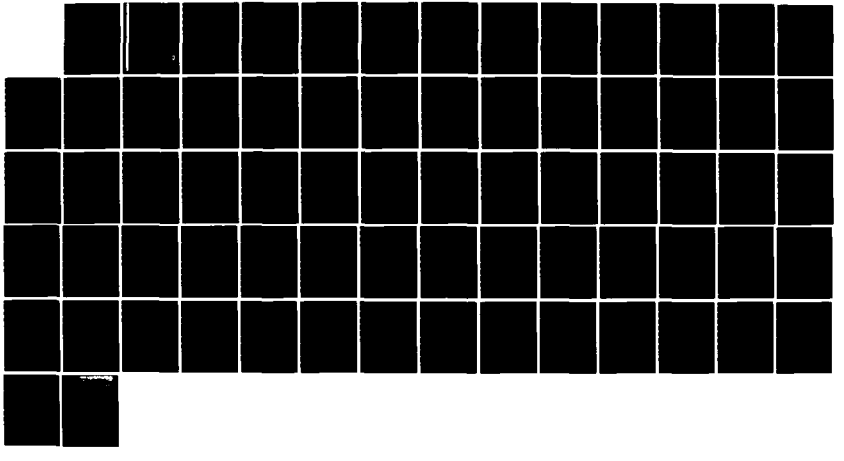

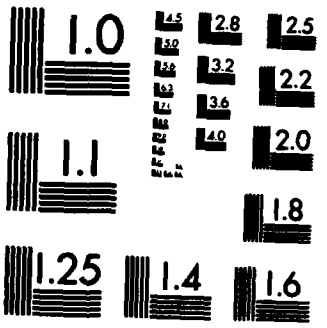

MICROWAVE LABORATORY REPORT NO. 84-7

MILLIMETER-WAVE TRAVELLING-WAVE IMPATT DIODE

TECHNICAL REPORT

YOSHIRO FUKUOKA and TATSUO ITOH

MAY 31, 1984

U.S. ARMY RESEARCH OFFICE

Contract No.: DAAG29-81-K-0053

UNIVERSITY OF TEXAS
DEPARTMENT OF ELECTRICAL ENGINEERING
AUSTIN, TEXAS 78712

APPROVED FOR PUBLIC RELEASE;
DISTRIBUTION UNLIMITED

SECURITY CLASSIFICATION OF THIS PAGE (When Data Entered)

REPORT DOCUMENTATION PAGE		READ INSTRUCTIONS BEFORE COMPLETING FORM
1. REPORT NUMBER ARO 17735.35-EL	2. GOVT ACCESSION NO. AD-A146 545	3. RECIPIENT'S CATALOG NUMBER
4. TITLE (and Subtitle) MILLIMETER-WAVE TRAVELLING-WAVE IMPATT DIODE		5. TYPE OF REPORT & PERIOD COVERED Technical Report 6. PERFORMING ORG. REPORT NUMBER
7. AUTHOR(s) Yoshiro Fukuoka and Tatsuo Itoh		8. CONTRACT OR GRANT NUMBER(s) DAAG 29-81-K-0053
9. PERFORMING ORGANIZATION NAME AND ADDRESS University of Texas at Austin P.O. Box 7728 Austin, Texas 78712		10. PROGRAM ELEMENT, PROJECT, TASK AREA & WORK UNIT NUMBERS
11. CONTROLLING OFFICE NAME AND ADDRESS U. S. Army Research Office Post Office Box 12211 Research Triangle Park, NC 27709		12. REPORT DATE 8/13/84 13. NUMBER OF PAGES 62
14. MONITORING AGENCY NAME & ADDRESS(if different from Controlling Office)		15. SECURITY CLASS. (of this report) Unclassified 15a. DECLASSIFICATION/DOWNGRADING SCHEDULE

16. DISTRIBUTION STATEMENT (of this Report)

Approved for public release; distribution unlimited.

17. DISTRIBUTION STATEMENT (of the abstract entered in Block 20, if different from Report)

18. SUPPLEMENTARY NOTES

The views, opinions, and/or findings contained in this report are those of the author(s) and should not be construed as an official Department of the Army position, policy, or decision, unless so designated by other documentation.

19. KEY WORDS (Continue on reverse side if necessary and identify by block number)

IMPATT DIODE, TRAVELLING WAVE, MILLIMETER-WAVE FREQUENCY

20. ABSTRACT (Continue on reverse side if necessary and identify by block number)

DD FORM 1 JAN 73 1473 EDITION OF 1 NOV 65 IS OBSOLETE

SECURITY CLASSIFICATION OF THIS PAGE (When Data Entered)

MICROWAVE LABORATORY REPORT NO. 84-7

MILLIMETER-WAVE TRAVELLING-WAVE IMPATT DIODE

TECHNICAL REPORT

YOSHIRO FUKUOKA and TATSUO ITOH

MAY 31, 1984

U.S. ARMY RESEARCH OFFICE

Contract No.: DAAG29-81-K-0053

UNIVERSITY OF TEXAS
DEPARTMENT OF ELECTRICAL ENGINEERING
AUSTIN, TEXAS 78712

ABSTRACT

A millimeter-wave travelling-wave IMPATT diode is studied. This device has a simple configuration and is suitable for monolithic integration. The travelling-wave structure permits oscillation of the IMPATT diode at a desired frequency without any external resonant circuit, making the whole system extremely simple. The theoretical analysis determines the condition under which gain is produced in the IMPATT device. A reasonable agreement is obtained with the experimental results.

TABLE OF CONTENTS

LIST OF FIGURES

Figure 13 Computed input admittance of the periodic IMPATT oscillator

LIST OF TABLES

CHAPTER 1 : INTRODUCTION

An impact avalanche transit time (IMPATT) diode is an attractive source at millimeter-wave (mm-wave) frequencies because it is capable of producing a large power. An IMPATT diode is a pn diode which utilizes the avalanche multiplication effect in the depletion layer under the breakdown condition to generate mm-wave energy. The size of the depletion layer thickness of an IMPATT diode is determined by its operation frequency. As the frequency becomes higher, a thinner depletion layer is required for efficient IMPATT operation. This, however, results in a smaller negative resistance for the same device area, which makes impedance matching to the external circuit difficult. One way to overcome this limitation is to shunt-resonate the large capacitance of the IMPATT diode. A travelling-wave structure with an appropriate length is one way of realizing the shunt resonance [1-3]. Fig. 1 shows a very simple single-drift travelling-wave IMPATT diode. The structure is elongated in one direction (the z direction) and the electromagnetic wave travelling along this direction draws energy from dc current by the IMPATT mechanism and is therefore amplified.

This type of IMPATT diode was first proposed by Midford et.al., [1]. They actually constructed a silicon (Si) single-drift deviced and tested it as an amplifier. One advantage of the travelling-wave IMPATT diode over the lumped construction is that it can be used as an oscillating source as well as a two-port amplifier depending on the

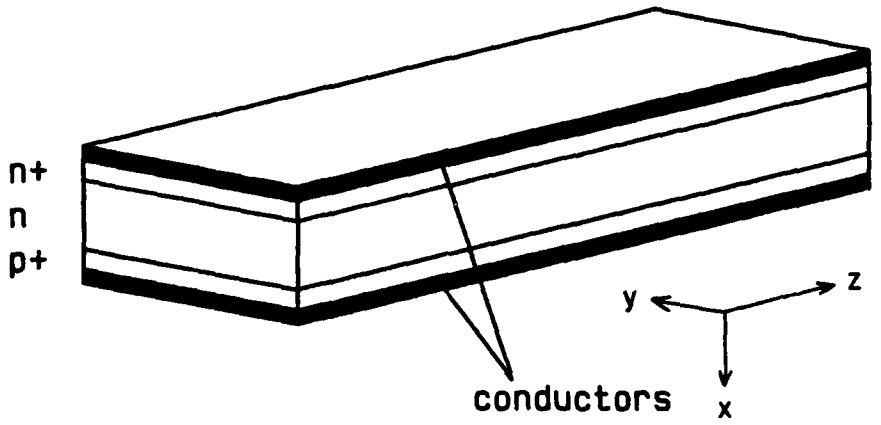

Figure 1 Schematic view of the single-drift travelling-wave IMPATT diode

length and the coupling condition to the external circuit. For example, if the device length were one half wavelength at the designated frequency and the both ends of the device were left open-circuited, then it would oscillate by itself at the desired frequency without an external resonant circuit. This configuration makes the whole circuit simple, and therefore this device is suitable for integrated circuit. On the other hand, if the device were connected to the external circuit with good impedance matching, then it would amplify the signal coming from one end. This amplifier also works in both directions, and the structure is again very simple.

The travelling-wave IMPATT diode has attractive features but not much work had done on it until the recent technological development in semiconductor processing. Molecular beam epitaxy (MBE) is capable of producing very thin uniformly doped semiconductor layers, which is necessary for a millimeter-wave IMPATT diode [4]. It is possible to make uniform 0.1 μm-thick layer over a 1 mm-long device using MBE technology, and experimental work shows that such a device generates a useful amount of power at mm-wave frequencies, 30 - 90 GHz [5].

Part II comprises a theoretical analysis of the travelling-wave IMPATT diode. All possible losses caused by the conductors as well as the semiconductors are included in the analysis since their contribution at mm-wave frequencies are not negligible. Under the small-signal assumption, numerical results have been obtained for Si single-drift and GaAs double-drift travelling-wave IMPATT diodes. Comparison with experimental results obtained by other authors shows good agreement.

CHAPTER 2 : TRAVELLING-WAVE IMPATT THEORY

A travelling-wave IMPATT diode contains several very thin semiconductor layers. This makes it feasible to assume that the diode is very wide compared to the thickness. The structure to be studied, therefore, reduces to a one-dimensional multilayered parallel-plate waveguide containing an active IMPATT medium. Fig. 2 shows the side view of the double-drift travelling-wave IMPATT diode. Materials change only in the x direction, and the electromagnetic wave is assumed to propagate in the z direction. In the y direction, both material constants and field components are assumed to be uniform. Under an appropriate reverse dc bias condition, avalanche breakdown occurs mainly along the pn junction at the center of the device. Charge carriers travel in the n and p regions at saturation velocities. If a single-drift travelling-wave IMPATT diode is considered, the two center regions (n and p) should be replaced with a single (n) material. Since this can be considered as a special case of the double-drift device, the theory is developed for the double-drift device.

In a multilayered structure, the dominant propagating mode is a TM mode. This mode has only the y component of the magnetic field and the x and z components of the electric field. This mode becomes a TEM mode if the material contained between two conductors is uniform and the conductors are perfect. However, the structure contains several different materials between conductors, and the conductors usually consist of

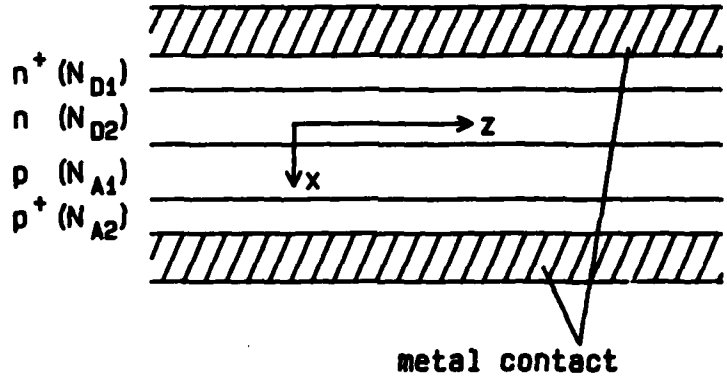

Figure 2 Side view of the double-drift travelling-wave IMPATT diode

a couple of different metals in order to form proper contacts. Therefore transverse magnetic (TM) propagation occurs in the entire structure, and establishes the required boundary conditions.

The analytical process is summarized as follows. A system of differential equations governing IMPATT behavior are first solved to determine the boundary of the space-charge region. For example, in the single-drift diode, the space-charge region extends from inside of the p+ region to the point near the nn+ boundary (Fig. 3). The wave equation is then solved in each layer including this active region. The tangential electric and magnetic fields must be matched at every boundary. The quantity obtained from the analysis is the propagation constant of the travelling wave. This is a complex quantity with which the gain and phase of the wave in the device can be investigated.

ANALYSIS OF THE SPACE-CHARGE REGION

The space-charge region consists of the avalanche region and the drift region, in which the dc electric field is strong enough so that the carrier electrons and holes travel at saturation velocities. In practice, if the pn junction is formed by two uniform p and n materials, then the avalanche and the drift regions can not be separated. In other words, these two processes occur simultaneously in the space-charge region. In order to physically separate these two regions, it is necessary to control the doping variation in the device (for example, the Read diode [6]). In the millimeter-wave IMPATT diode, however, it is

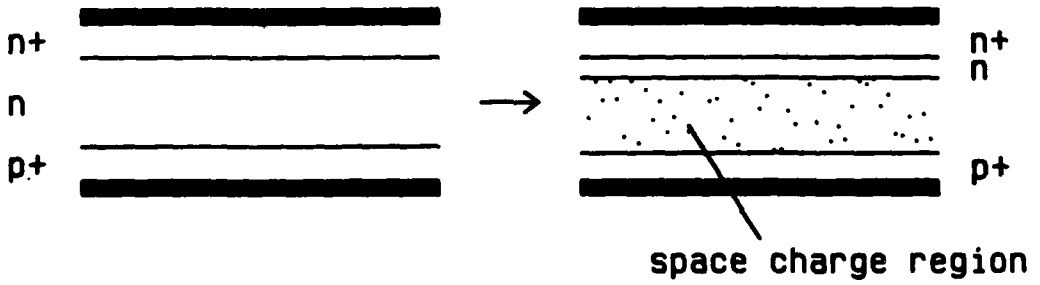

Figure 3 Space-charge region formed in the single-drift IMPATT diode

usually difficult to control the variation of the doping level in each layer near the pn contact since the entire structure is very small. Therefore, the avalanche and drift regions can not physically be separated. For this reason, we have to treat the space-charge region without separating it into two different regions.

The differential equations governing the IMPATT medium are as follows [7]:

$$\nabla^2\vec{E} - \nabla(\nabla\cdot\vec{E}) - \mu\varepsilon\frac{\partial^2\vec{E}}{\partial t^2} - \mu\frac{\partial\vec{J}_c}{\partial t} = 0 \qquad (1)$$

$$\nabla\cdot\vec{E} = \frac{q}{\varepsilon}\left(N_D - N_A + p - n \right) \qquad (2)$$

$$\frac{\partial n}{\partial t} = \frac{1}{q}\left(\nabla\cdot\vec{J}_n + \alpha|J_n| + \beta|J_p| \right) \qquad (3)$$

$$\frac{\partial p}{\partial t} = \frac{1}{q}\left(-\nabla\cdot\vec{J}_p + \alpha|J_n| + \beta|J_p| \right) \qquad (4)$$

where

$\vec{E}$ = electric field

$\vec{J}_c$ = conduction current

$\vec{J}_n$ = electron current

$\vec{J}_p$ = hole current

N_D = donor impurity concentration

N_A = acceptor impurity concentration

n = electron concentration

p = hole concentration

α = generation rate for electrons

β = generation rate for holes

q = unit charge

ε = permittivity

μ = permeability

The first two equations are derived from the Maxwell's equations and the remaining equations represent continuity of the current and charges. The generation rate (ionization rate) α and β are functions of the magnitude of the electric fields and the relations are given by [8]

$$\alpha = A \exp \{ - [\frac{b}{|E(x)|}]^m \} \qquad (5)$$

The values of A, b, and m appearing in these equations are given in Table 1 for Si and GaAs. The generation rate is the rate of producing electron-hole pairs which is caused by avalanche multiplication.

To solve the differential equations (1) through (4), we have to make a few assumptions. First we separate each variable into dc and ac parts. It is assumed that the ac signal is much smaller than the dc value, and we take only the first-order sinusoidal term in the ac component. Also, we assume a travelling-wave form for the ac term which has a propagation constant γ. For example, the x component of the electric field is written as

$$E_x = E_{xDC} + \tilde{E}_x \, e^{j\omega t - \gamma z} \qquad (6)$$

The dc bias voltage is applied only in the vertical direction (x direction). Therefore we retain only the x components of the dc quantities. Also, the carrier velocities in this direction are limited to the saturation velocities by the high dc electric field in the IMPATT medium. The relation between the x component of the current density and the carrier concentration can simply be described as:

$$J_{nx} = qnv_{ns}$$

$$J_{px} = qpv_{ps} \qquad (7)$$

Table 1 Parameters of generation rates α and β

material	electrons A	electrons b	holes A	holes b	m
Si	3.8×10^8	1.75×10^8	2.25×10^9	3.26×10^8	1
GaAs	3.5×10^7	6.85×10^7	3.5×10^7	6.85×10^7	2

where v_{ns} and v_{ps} are the saturation velocities of the electrons and the holes, respectively, in the semiconductor material.

Using these relations, the differential equations governing the dc components are written as follows:

$$\frac{dE_{xDC}}{dx} = \frac{q}{\varepsilon}\left(N_D - N_A + p - n \right) \qquad (8)$$

$$\frac{dJ_{nxDC}}{dx} + \alpha J_{nxDC} + \beta J_{pxDC} = 0 \qquad (9)$$

$$\frac{dJ_{pxDC}}{dx} - \alpha J_{nxDC} - \beta J_{pxDC} = 0 \qquad (10)$$

By adding eqs. (9) and (10), we can obtain:

$$J_{nxDC} + J_{pxDC} = J_o \qquad (11)$$

where J_o is a constant. Physically, J_o represents the total dc bias current flowing in the IMPATT diode. This is an arbitrary constant and can be externally set to any value.

The differential equations for the ac components are obtained as follows:

$$\frac{d^2\tilde{E}_x}{dx^2} = \frac{1}{\varepsilon}\left(\frac{1}{v_{ps}}\frac{d\tilde{J}_{px}}{dx} - \frac{1}{v_{ns}}\frac{d\tilde{J}_{nx}}{dx}\right) + j\omega\mu\left(\tilde{J}_{nx} + \tilde{J}_{px}\right) - \left(\gamma^2 + \omega^2\mu\varepsilon\right)\tilde{E}_x \qquad (12)$$

$$\frac{d\tilde{E}_x}{dx} + \gamma\tilde{E}_z = \frac{1}{\varepsilon}\left(\frac{\tilde{J}_{px}}{v_{ps}} - \frac{\tilde{J}_{nx}}{v_{ns}}\right) \qquad (13)$$

$$\frac{j\omega}{v_{ns}}\tilde{J}_{nx} = \frac{d\tilde{J}_{nx}}{dx} - \gamma\tilde{J}_{nz} + \alpha\tilde{J}_{nx} + \beta\tilde{J}_{px} + \left(J_{nxDC}\alpha' + J_{pxDC}\beta'\right)\tilde{E}_x \qquad (14)$$

$$\frac{j\omega}{v_{ps}}\tilde{J}_{px} = -\frac{d\tilde{J}_{px}}{dx} + \gamma\tilde{J}_{pz} + \alpha\tilde{J}_{nx} + \beta\tilde{J}_{px} + \left(J_{nxDC}\alpha' + J_{pxDC}\beta'\right)\tilde{E}_x \qquad (15)$$

where α' and β' are the derivatives with respect to the electric field. Since there is no dc bias voltage applied in the z direction, we can use

the following relations between the z component of the current density and the electric field:

$$\tilde{J}_{nz} = \sigma_n \tilde{E}_z$$

$$\tilde{J}_{pz} = \sigma_p \tilde{E}_z \qquad (16)$$

where σ_n and σ_p are the conductivities due to the electrons and holes, respectively. These conductivities can be calculated from the distribution of the dc current densities:

$$\sigma_n = q\mu_n n = \mu_n \frac{J_{nxDC}}{v_{ns}}$$

$$\sigma_p = \mu_p \frac{J_{pxDC}}{v_{ps}} \qquad (17)$$

where μ_n and μ_p are the mobilities of electrons and holes, respectively. Since the z component of the electric field can be expressed by eq. (13), eqs. (14) and (15) become:

$$\frac{d\tilde{J}_{nx}}{dx} = \left[\frac{1}{v_{ns}} \left(j\omega + \frac{\sigma_n}{\varepsilon} \right) - \alpha \right] \tilde{J}_{nx} - \left(\frac{1}{v_{ps}} \frac{\sigma_n}{\varepsilon} + \beta \right) \tilde{J}_{px} - \left(J_{nxDC}\alpha' + J_{pxDC}\beta' \right) \tilde{E}_x + \sigma_n \frac{d\tilde{E}_x}{dx} \qquad (18)$$

$$\frac{d\tilde{J}_{px}}{dx} = \left[- \frac{1}{v_{ps}} \left(j\omega + \frac{\sigma_p}{\varepsilon} \right) + \beta \right] \tilde{J}_{px} + \left(\frac{1}{v_{ns}} \frac{\sigma_p}{\varepsilon} + \alpha \right) \tilde{J}_{nx} + \left(J_{nxDC}\alpha' + J_{pxDC}\beta' \right) \tilde{E}_x + \sigma_p \frac{d\tilde{E}_x}{dx} \qquad (19)$$

The ac equations to be solved are eqs. (12), (18) and (19).

BOUNDARY CONDITIONS

In order to solve the above differential equations, we have to specify all the boundary conditions. The boundaries of the space-charge region are not yet known and must be determined by applying the dc boundary conditions. The dc electric field becomes negligible outside of the space-charge region since the outer regions are much more conductive

than the space-charge region, which is basically a depletion layer. At the space-charge region boundary in the n layer, the current consists of only electron current. Also, at the p layer boundary, the current consists of only hole current. By applying these conditions, both boundaries of the space-charge region can be determined.

Once we have found the boundaries of the space-charge region, we can apply boundary conditions to the ac quantities. The boundary conditions on the ac current densities are the same as in the dc case:

$$\tilde{J}_{px} = 0 \qquad \text{at the boundary in n layer}$$

$$\tilde{J}_{nx} = 0 \qquad \text{at the boundary in p layer} \qquad (20)$$

The tangential field components, H_y and E_z, must be matched to the outside regions.

Outside of the space-charge region, we have conductive materials which do not contribute to producing rf energy. In such a region, we can write the field components as

$$H_y = A_i e^{j\xi_i x} + B_i e^{-j\xi_i x}$$

$$E_z = \frac{\xi_i}{\omega\varepsilon_i} \left(A_i e^{j\xi_i x} - B_i e^{-j\xi_i x} \right) \qquad (21)$$

where

$$\xi_i^2 = \gamma^2 + \omega^2 \varepsilon_i \mu$$

and A_i and B_i are constants determined from the boundary conditions. These field components can be matched at each boundary of the metal and semiconductors, which leads to an eigenvalue equation for the propagation constant. At the space-charge region boundaries, these field quantities are transformed into field quantities used in the ac equations (12), (18) and (19) by using the following relations.

$$\gamma \tilde{H}_y = j\omega\varepsilon \tilde{E}_x + \tilde{J}_{px} + \tilde{J}_{nx}$$

$$\gamma \tilde{E}_z = \frac{d\tilde{E}_x}{dx} - \frac{1}{\varepsilon}\left(\frac{\tilde{J}_{px}}{v_{ps}} - \frac{\tilde{J}_{nx}}{v_{ns}}\right) \qquad (22)$$

The solutions of the dc and ac differential equations are obtained by Runge-Kutta integration. The second-order equation (12) is formally separated into two first-order equations, and since the ac equations are complex, they are separated into real and imaginary parts and treated as different equations. Iteration is then performed until all of the above boundary conditions are satisfied. The fourth- and fifth-order Runge-Kutta routine RKF45 in the numerical analysis library at The University of Texas was used extensively. This routine was first

written by H. A. Watts and L. F. Shampine at Sandia Laboratories and can be found in [9]. Also the system nonlinear equation solver, ZSPOW, and the complex root-search routine, ZANLYT, in IMSL were both used to match the boundary conditions.

CHAPTER 3 : SINGLE-DRIFT TRAVELLING-WAVE IMPATT DIODE

The theoretical analysis was first applied to the simple single-drift travelling-wave IMPATT diode (n+np+) which had been analyzed by Franz using a different method [7]. The material used is Si and all the layers except the depletion region (n layer) are assumed to be perfect conductors. The dimensions and the other parameters are shown in Table 2. In this particular structure, the entire n region becomes the space-charge region under operating conditions. Therefore the boundary of the space-charge region is already known. The remaining boundary conditions to be satisfied are the conditions on the current densities and the electric field: the z component of the electric field is required to be zero at the n+n and np+ boundaries.

The calculated results are shown in Fig. 4. In Fig. 4a, the gain produced in the diode is shown for various dc current densities. The upper half of the figure indicates gain and the lower half indicates loss. As the dc current density increases, the gain also increases. Each curve has a discontinuity at a certain frequency. For example, when the dc current density is 1×10^7 A/m^2, a large loss suddenly becomes a large gain around 6.5 GHz. The frequency of the discontinuity in the gain corresponds to the avalanche resonant frequency where the negative resistance of the conventional lumped IMPATT diode has a discontinuity [10,11]. The maximum gain constant is obtained just above this discontinuity. In practice, however, if the device is operated at the frequency

Table 2 Parameters used in the calculation of Si single-drift travelling-wave IMPATT diode

dielectric constant (ε_r)	11.8
donor concentration (N_D)	2.2×10^{21} /m^3
depletion layer thickness	7.0 μm
saturation velocity (v_s)	10^5 m/sec

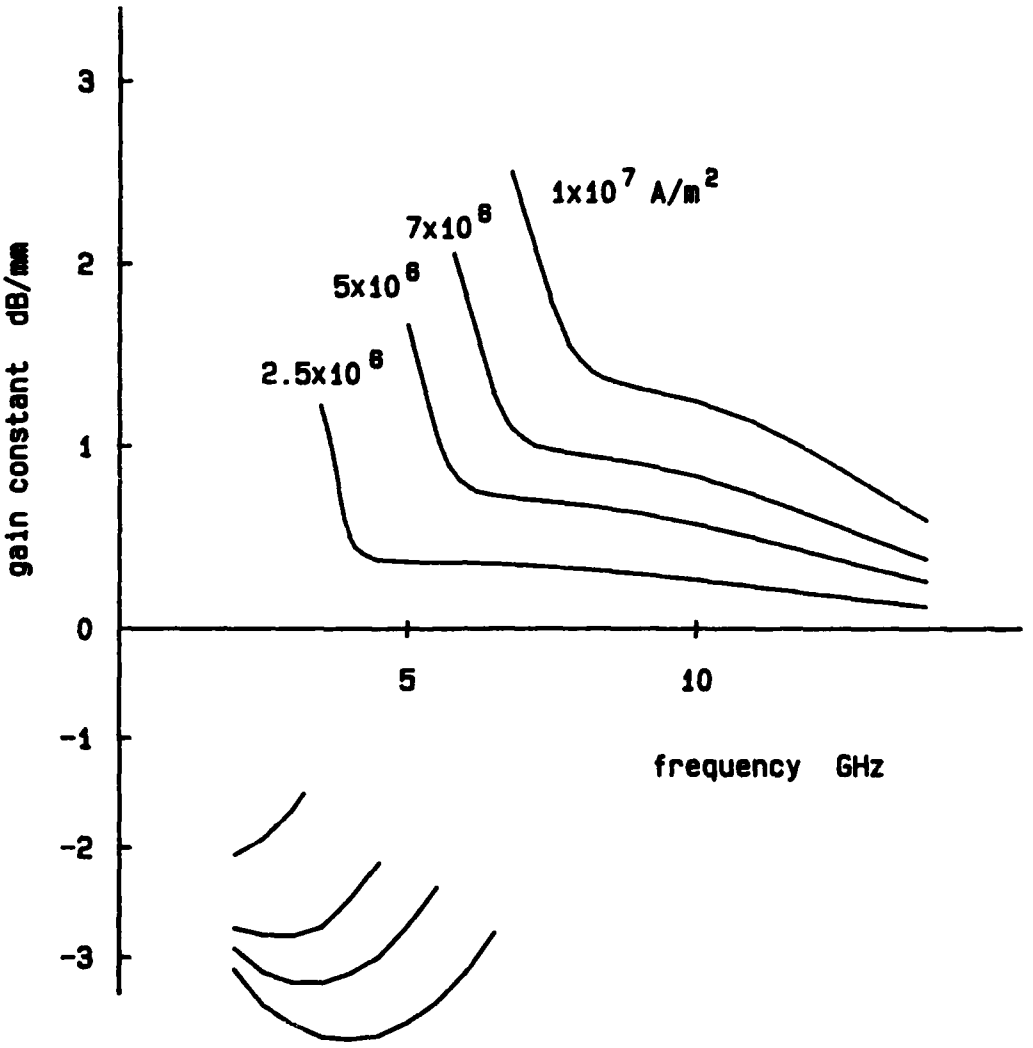

Figure 4a Gain constant versus frequency in the single-drift travelling-wave IMPATT diode : Parameter is DC bias current density.

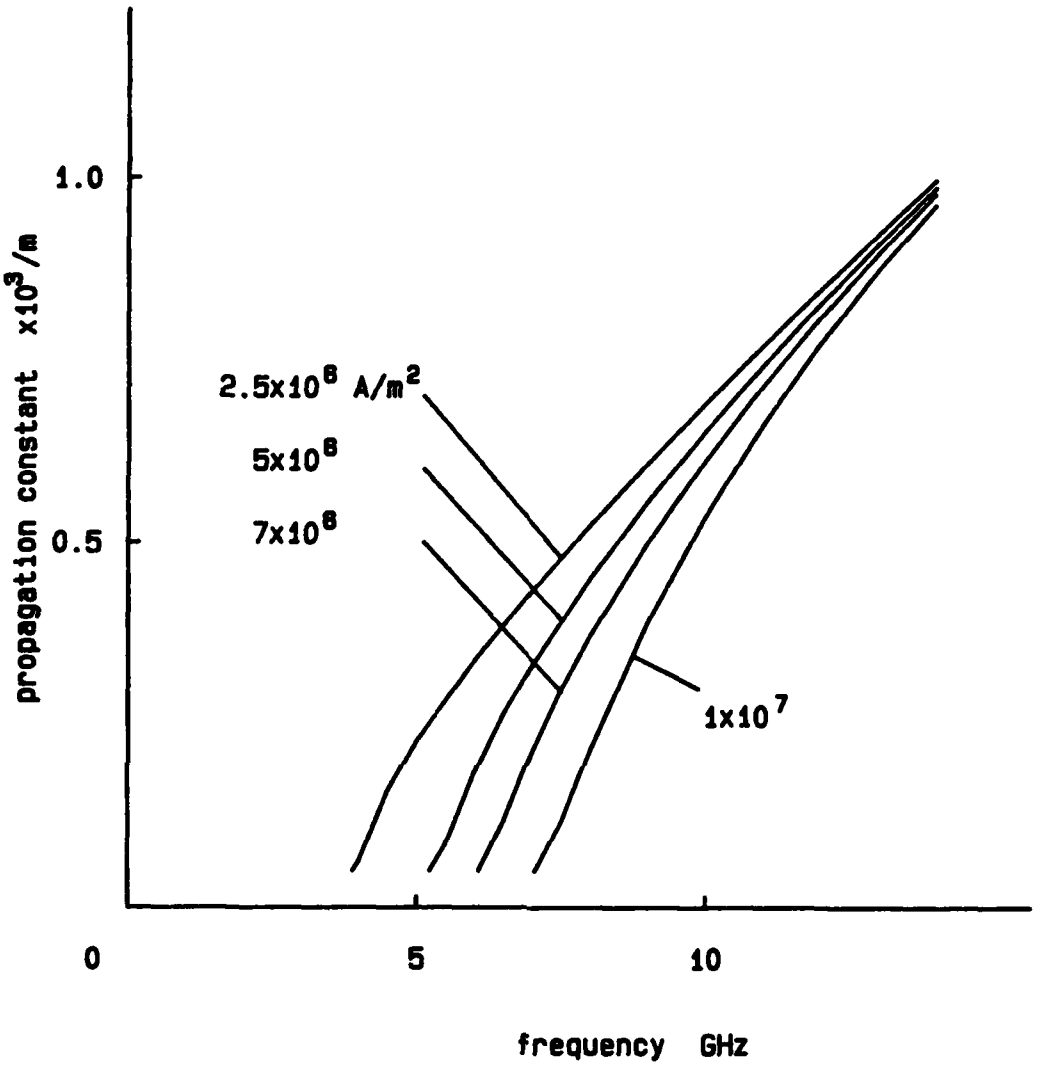

Figure 4b Propagation constant versus frequency in the single-drift travelling-wave IMPATT diode : Parameter is DC bias current density.

just above the avalanche frequency, the operating point moves back and forth between the regions of gain and loss because of the large-signal nature of the actual device. Therefore, the device can not generate a stable net gain. Hence the operating point should be chosen well above the avalanche resonance frequency. This theoretical discontinuity occurs because of the small-signal assumption, and therefore the theory can not be used to predict the behavior of the device near avalanche resonance. If the behavior of the device near the avalanche resonance is to be investigated, a large-signal analysis needs to be done.

The propagation constant is shown in Fig. 4b. The curves are shown only at frequencies higher than the avalanche resonance frequency. The phase velocity of the travelling wave approaches the velocity of a TEM wave in lossless Si material (ε_r=11.8) as the frequency increases. Also the phase velocity increases as avalanche resonance is approached.

These results can be compared to those obtained theoretically by Franz [7]. The theoretical values of gain are much smaller than Franz's while the behavior of the propagation constants agrees qualitatively. The difference is due to different simplifying assumptions. Fig. 5 shows the dc solution of the present device. Fig. 5b indicates that avalanche multiplication occurs in more than half of the entire depletion region. This means that the assumption made by Franz that the avalanche region is infinitesimally thin and the entire space-charge region can be treated as a drift region should not be used. Actually carrier drift and avalanche multiplication occur simultaneously. It is not necessary to distinguish these two regions in this analysis. The effect of the loss caused by the inactive regions will be discussed in the next chapter.

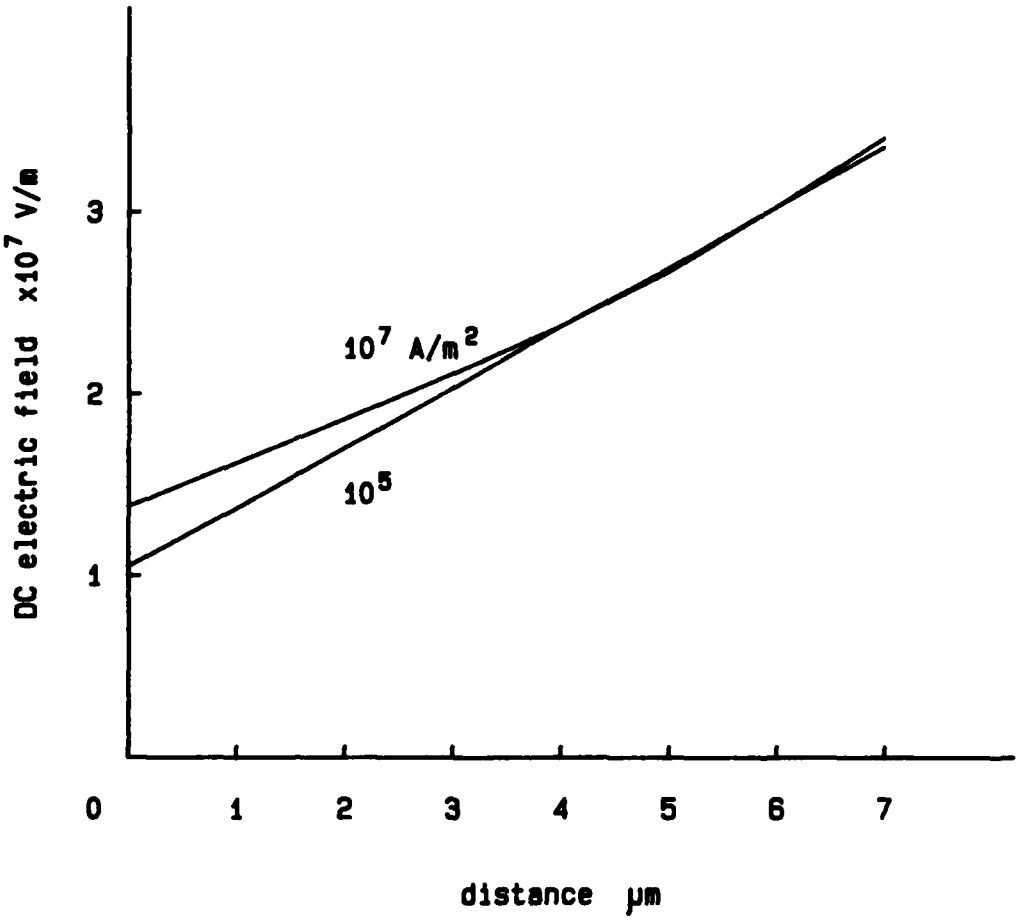

Figure 5a Solution of the DC equation : DC electric field is plotted as a function of the distance from the n^+n junction. Parameter is DC bias current density.

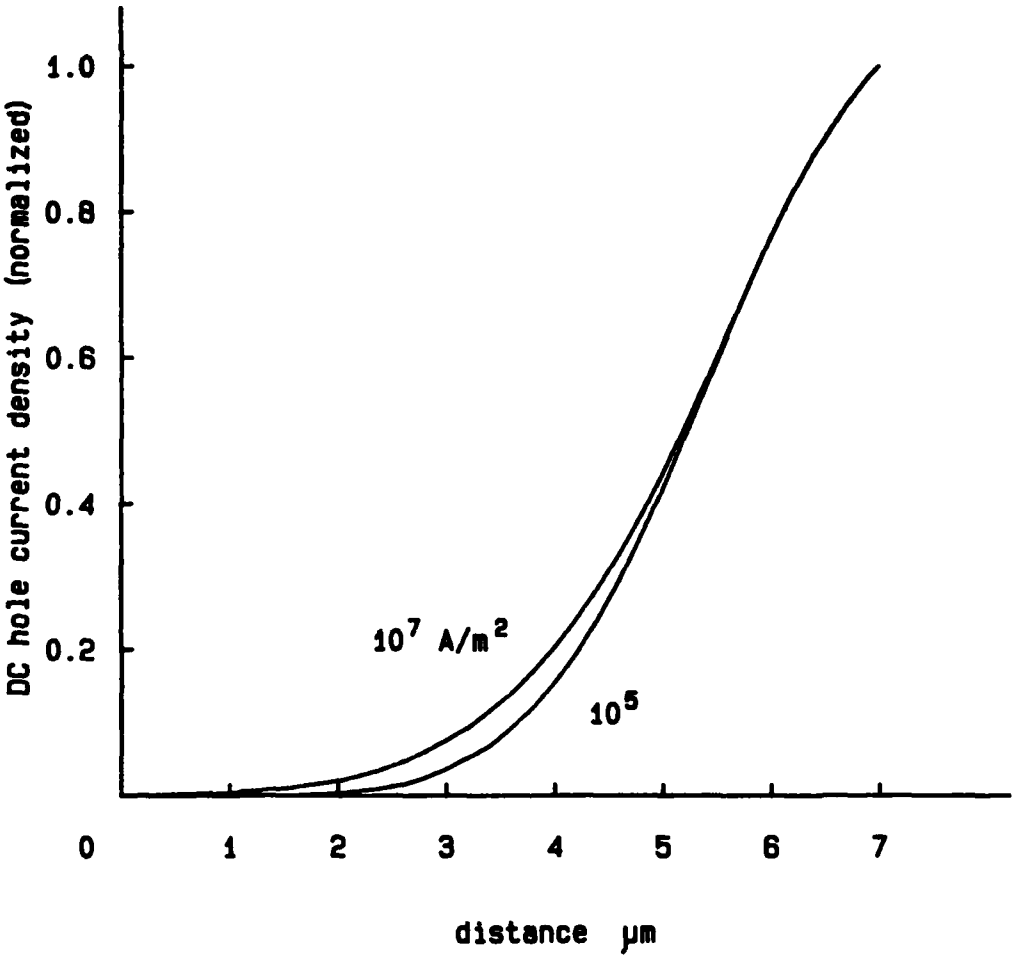

Figure 5b Solution of the DC equation : DC hole current density is plotted as a function of the distance from the n^+n junction. Parameter is DC bias current density.

CHAPTER 4 : DOUBLE-DRIFT TRAVELLING-WAVE IMPATT DIODE

A double-drift IMPATT diode is potentially capable of producing more power than a single-drift diode [12-14]. The depletion region of the double-drift diode consists of two layers (p and n). The dc electric field is maximum at the center junction (pn junction) and therefore avalanche multiplication primarily occurs in this region.

The parameters chosen for the numerical calculations are shown in Table 3. The structure consists of 8 layers and is very similar to the one used in the experiment of Bayraktaroglu et.al. [5]. The inactive layers are treated as lossy dielectric layers and their effect is taken into account.

The computed results for gain and propagation constants are presented in Fig. 6. As frequency decreases and approaches avalanche resonance, the gain increases and the phase velocity of the wave increases. In these figures, dotted lines indicate the results for the special case that the depletion region is replaced by a lossless material, where slow-wave propagation becomes evident. Each curve asymptotically approaches the dotted line at high frequencies, since the device becomes inefficient there and deviates from IMPATT operation.

Fig. 7 compares the present theory and the experimental results obtained by [5]. The device was used as an oscillator with one end open and the other terminated in a short. In the figure, white circles (o) show the actual device lengths and the oscillation frequency obtained in

Table 3 Parameters used in the calculation of GaAs double-drift travelling-wave IMPATT diode

material	thickness (μm)	doping level ($/m^3$)	conductivity (S/m)
Au	7.0	-	4.3×10^{7}
Ti	0.1	-	1.8×10^{6}
n+ GaAs	0.2	5.0×10^{24}	6.8×10^{5}
n GaAs	0.3	1.5×10^{23}	2.0×10^{4}
p GaAs	0.3	1.5×10^{23}	9.6×10^{2}
p+ GaAs	0.2	5.0×10^{24}	3.2×10^{4}
Ti	0.1	-	1.8×10^{6}
Au	7.0	-	4.3×10^{7}

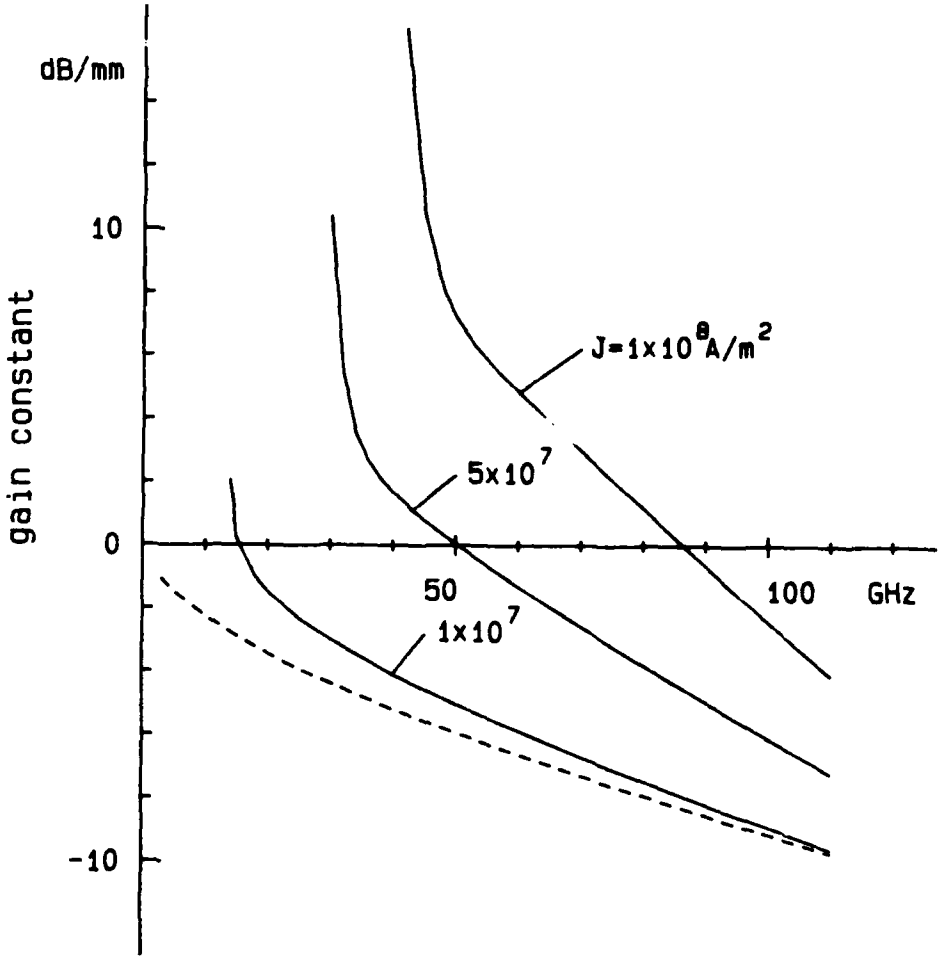

Figure 6a Gain constant versus frequency in the double-drift travelling-wave IMPATT diode : Parameter is DC bias current density.

– – – – : Active region is replaced by loss-less GaAs material.

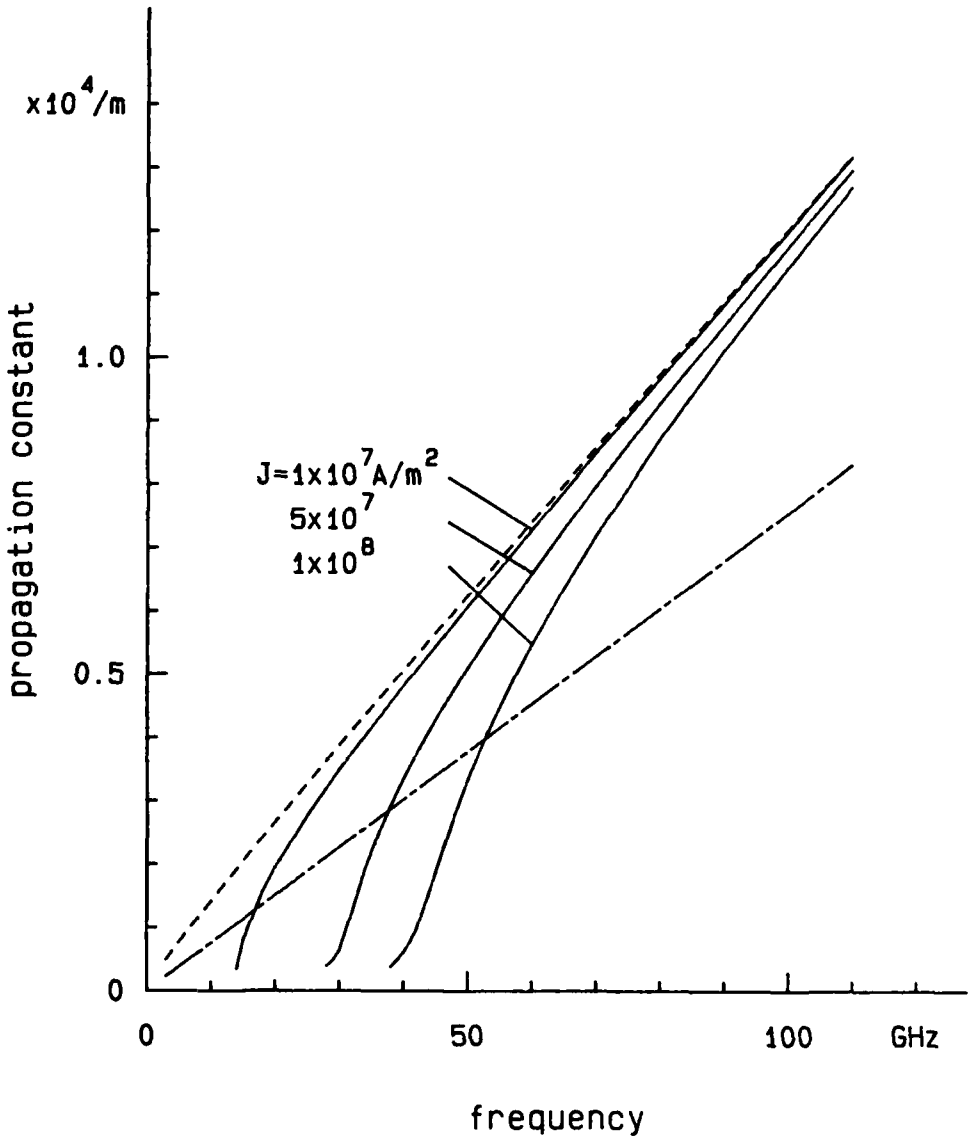

Figure 6b Propagation constant versus frequency in the double-drift travelling-wave IMPATT diode : Parameter is DC bias current density.

– – – – : Active region is replaced by lossless GaAs material.

—·—·— : $\sqrt{13}\ k_o$

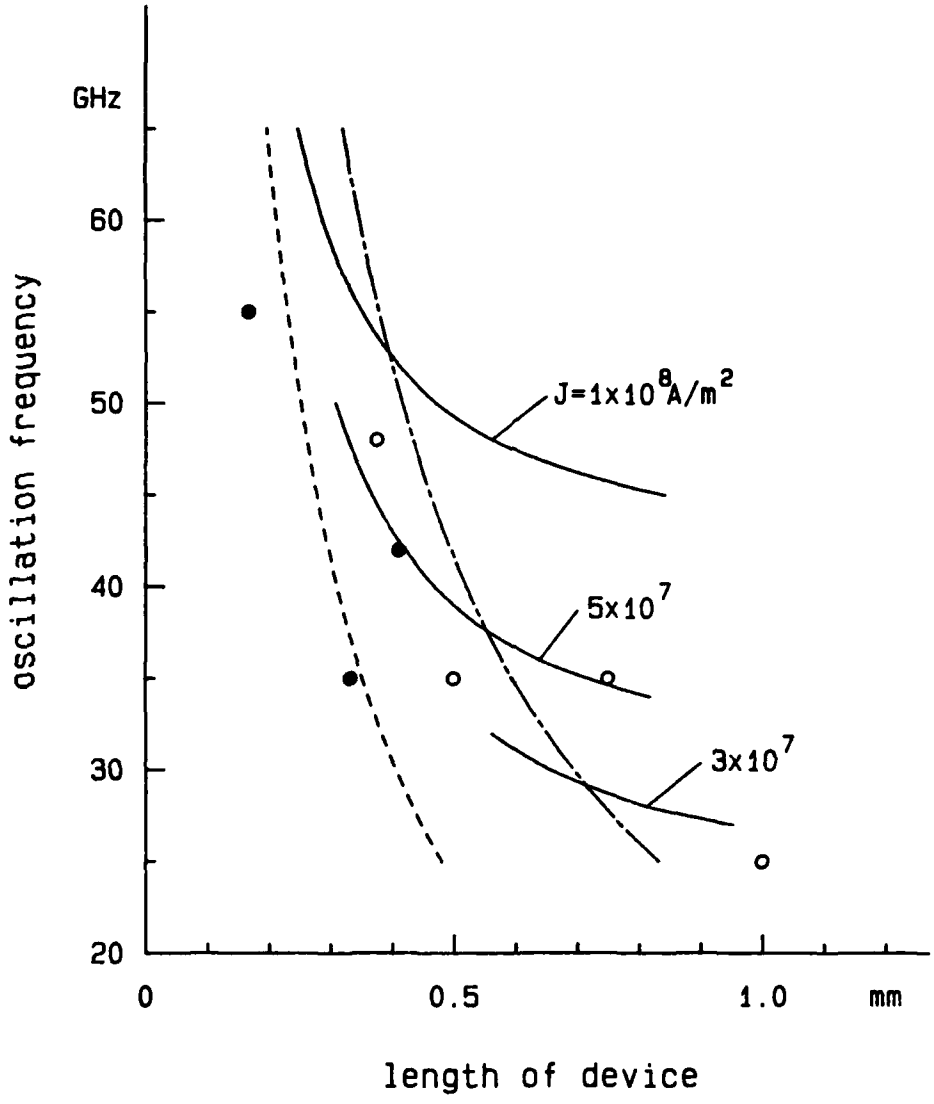

Figure 7 Comparison between experiment and theory : Solid lines represent the region where net gain is produced in the device.

– – – – : Active region is replaced by loss-less GaAs material.

—·—·— : $\sqrt{13}\ k_o$

the experiment, and black dots (•) show one-third of the actual device length (i.e., the device is considered to be oscillating at three-quarter wavelength). The three solid curves indicate the theoretical quarter wavelength where net gain is produced in the device. They are in good agreement except for two black dots where higher order resonance ($3\lambda/4$) takes place. In these cases, the actual terminating conditions might have a more dominant effect on the oscillation frequencies (i.e., not quite open circuit).

Fig. 8 shows how gain changes with respect to the dc current. As the dc current increases, the gain also increases but suddenly goes to a large loss below a critical bias point. This fact qualitatively agrees with the results of power measurements for conventional IMPATT diodes [4].

The oscillation frequency of the double-drift travelling-wave IMPATT diode is plotted with respect to the dc bias current in Fig. 9. The device length is fixed at 30 mils. Circles are the experimental results obtained by Bayraktaroglu [15]. Our theoretical curve closely follows them. In their experiment, a mode jump was observed around $J_o=8\times10^7$ A/m^2, although the theory shows continuous transition. In order to investigate this phenomenon, it is really necessary to include the effect of the coupling to the external circuits. In the figure, the dotted curve shows the oscillation frequency if the propagation constant is equal to that of TEM wave in a lossless GaAs material ($\varepsilon_r=13.0$). Therefore, the theoretical and experimental results show the fast wave nature of the travelling-wave IMPATT diode.

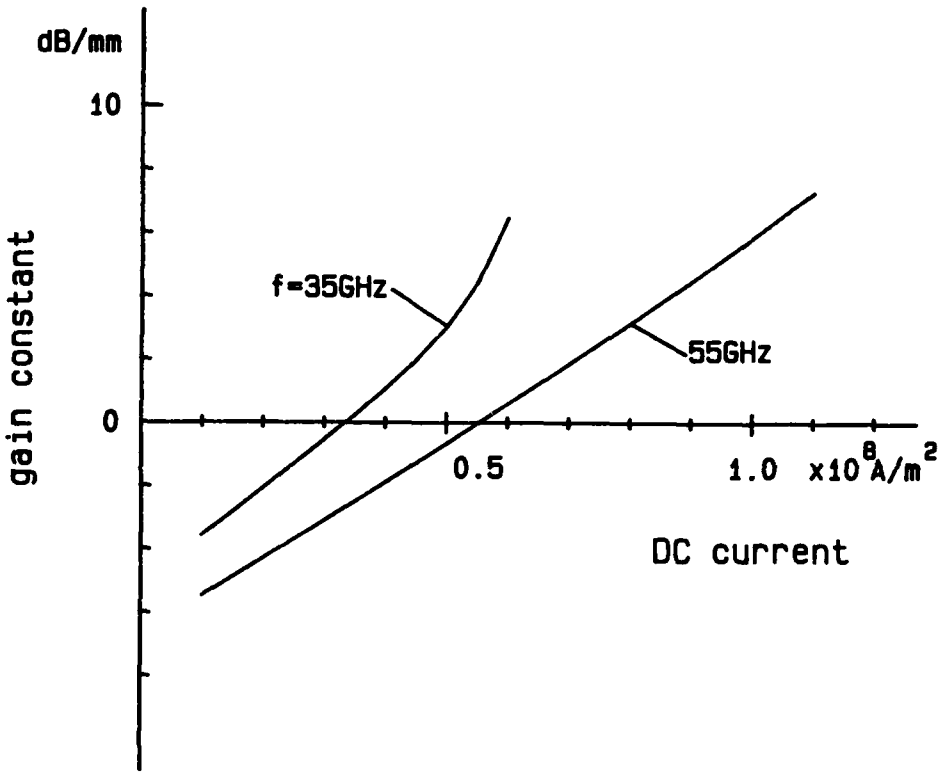

Figure 8 Gain constant versus DC bias current

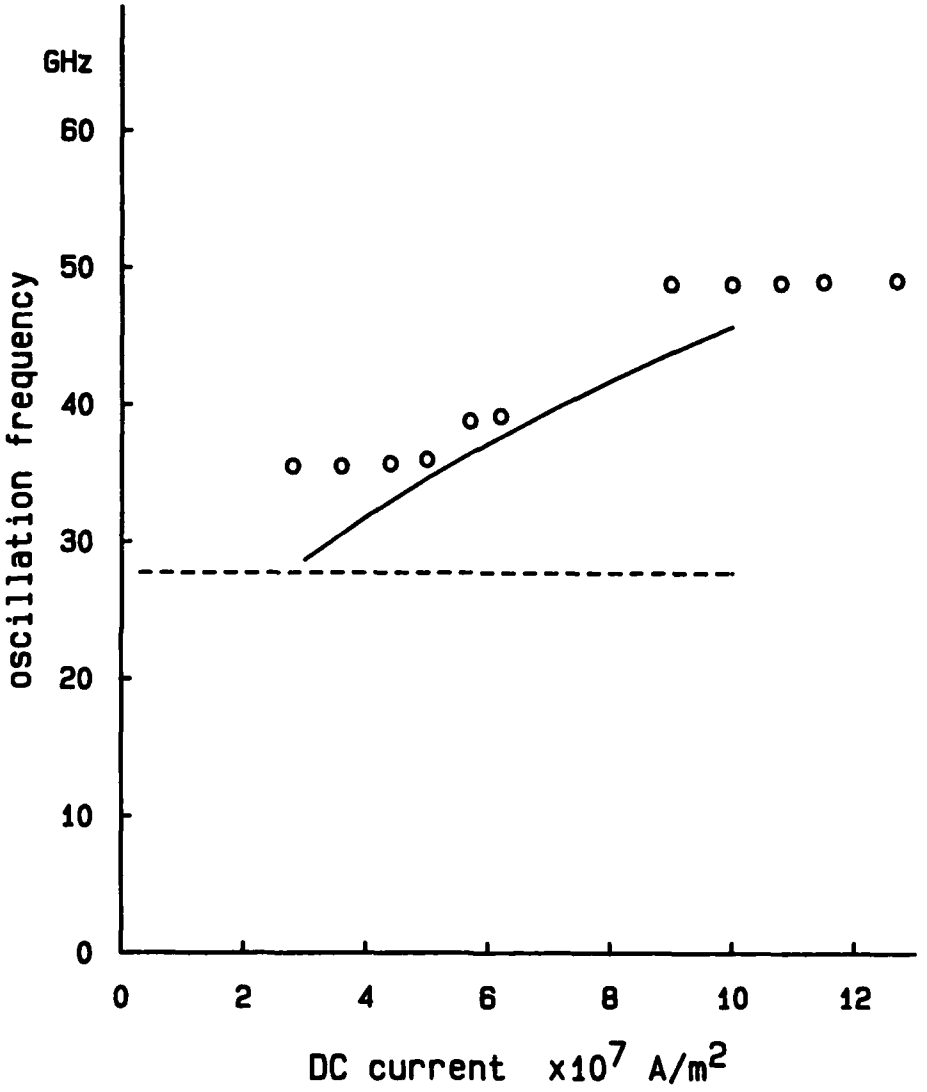

Figure 9 Comparison between experiment and theory :
Device length is 30 mils.
– – – – : $\beta = \sqrt{13}\, k_0$

CHAPTER 5 : PERIODIC IMPATT OSCILLATOR

So far, the discussion pertains only to the uniformly distributed IMPATT diode. It was shown that such a diode produces gain in the electromagnetic wave travelling along the pn junction. Such a diode is required to have extremely uniform semiconductor layers in order to have the same breakdown voltage over the diode area.

A travelling-wave IMPATT oscillator can also be realized by using a conventional TEM parallel-plate waveguide loaded periodically with lumped IMPATT diodes. This structure is shown in Fig. 10. Since each diode has a small area, it is easy to fabricate. Also, the structure includes the resonant circuit if appropriately cut and terminated. Therefore, we again do not need any external resonant circuit, and the entire system is kept simple.

In this chapter, a simple analysis of the periodic IMPATT oscillator is presented. The structure is basically modeled by a transmission line loaded with IMPATT impedances. The effect of the supporting metal posts are also included by calculating the inductance of the post. Some preliminary results are shown in the last section of this chapter.

CALCULATION OF THE POST IMPEDANCE

The parallel-plate waveguide loaded periodically with IMPATT

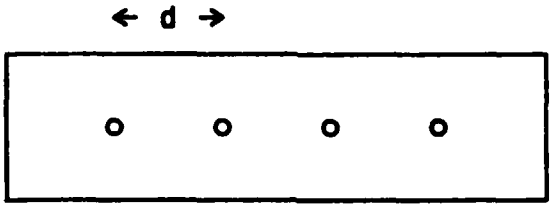

a

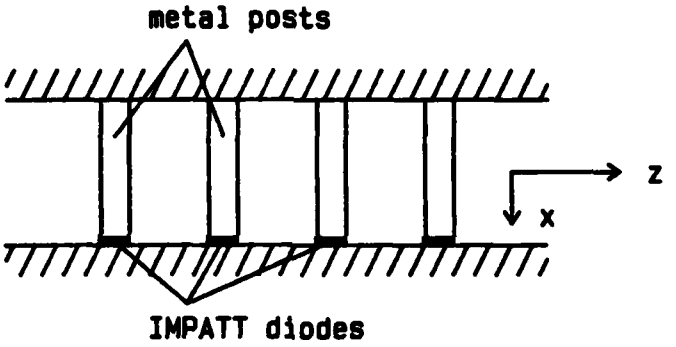

b

Figure 10 a Top view of the periodic IMPATT oscillator

b Side view

diodes is modeled by an equivalent transmission line loaded with impedance Z_p. The impedance Z_p is a sum of the ac IMPATT impedance and the metal post reactance. In this work, we treat the IMPATT diode as a lumped element, and the electric field component and current density are assumed to be oriented in the x-direction. The governing dc equations are the same as those developed in Chapter 2, i.e., (8), (9) and (10). The ac equations have simpler forms as follows:

$$\frac{d\tilde{E}}{dx} = \frac{1}{\varepsilon}\left\{\left(\frac{1}{v_{ps}} + \frac{1}{v_{ns}}\right)\tilde{J}_p - \frac{\tilde{J}}{v_{ns}} + \frac{j\omega\varepsilon}{v_{ns}}\tilde{E}\right\} \qquad (23)$$

$$\frac{d\tilde{J}_p}{dx} = \left(\beta - \alpha - \frac{j\omega}{v_{ps}}\right)\tilde{J}_p + \alpha\tilde{J}_{ac}$$

$$+ \left(J_{nDC}\alpha' + J_{pDC}\beta' - j\omega\varepsilon\alpha\right)\tilde{E} \qquad (24)$$

These equations are solved in a similar way to the previous analysis of the travelling-wave IMPATT diode. The ac electric field is then integrated over the entire IMPATT region to give the ac voltage, from which we can obtain the ac impedance of the diode.

The metal-post reactance needs to be calculated. Since the thickness of the IMPATT diode is much smaller than the length of the sup-

porting metal post, we can not neglect the effect of the reactance of the post. The metal post is assumed to be uniform in diameter. We use the conventional mode-matching technique to calculate the first-order inductance of the post [16]. The cross-sectional view of the waveguide model is shown in Fig. 11. The post is assumed to be located at z=0. A magnetic wall is placed on both sides and the field around the metal post can be expanded as follows:

$$E_y = \sum_{m=0}^{\infty} A_m \cos\frac{m\pi x}{a} e^{-\gamma_m |z|} \qquad (25)$$

$$H_x = \frac{1}{j\omega\mu} \sum_{m=0}^{\infty} -\gamma_m A_m \cos\frac{m\pi x}{a} e^{-\gamma_m |z|} \, \mathrm{sgn}(z) \qquad (26)$$

where

$$\gamma_m = \sqrt{\left(\frac{m\pi}{a}\right)^2 - k^2}$$

The assumption of continuity of H_x at z=0 gives:

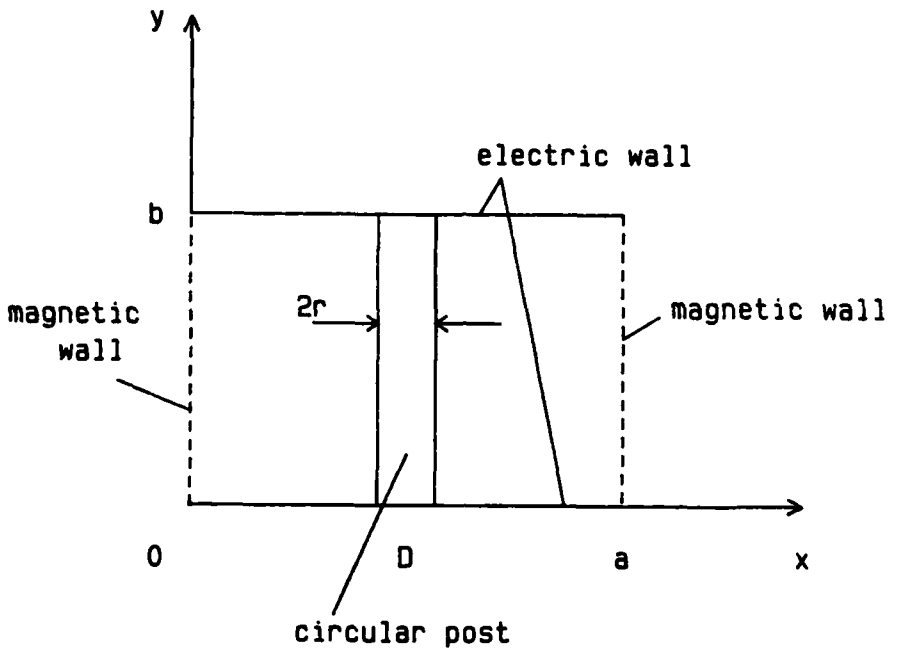

Figure 11 Cross-sectional view of the analytical model for the calculation of the metal-post reactance

$$-\frac{2}{j\omega\mu}\sum_{m=0}^{\infty} A_m \gamma_m \cos\frac{m\pi x}{a} = I\,\delta(x-D) \qquad (27)$$

where I is the current flowing on the metal post and $\delta(x)$ is the Dirac delta function. Using Fourier analysis, we can obtain A_m and hence:

$$E_y = \sum_{m=0}^{\infty} -\frac{j\omega\mu}{\gamma_m a} I \cos\frac{m\pi D}{a} \cos\frac{m\pi x}{a} e^{-\gamma_m |z|} \qquad (28)$$

We now assume that the incident wave is:

$$E_i = e^{-\gamma_o z}$$

The tangential electric field on the surface of the metal post must equal zero. We only choose one point (x=D+r, z=0) to do this:

$$1 - \frac{j\omega\mu}{a} I \sum_{m=0}^{\infty} \frac{1}{\gamma_m} \cos\frac{m\pi D}{a} \cos\frac{m\pi(D+r)}{a} = 0 \qquad (29)$$

Hence we can obtain the expression of the current I:

$$I = \frac{2a}{j\omega\mu}\left[\sum_{m=0}^{\infty}\left\{\cos\frac{m\pi r}{a}+\cos\frac{2m\pi D}{a}\right\}/\gamma_m\right]^{-1} \qquad (30)$$

Using this result, the impedance of the post jX_o is

$$X_o = \frac{k}{4}\left\{-\frac{a}{\pi}\log\left(4\sin\frac{\pi r}{2a}\sin\frac{\pi D}{a}\right) + \sum_{m=1}^{\infty}\left(1+\cos\frac{2m\pi D}{a}\right)\left(\frac{1}{\gamma_m}-\frac{a}{m\pi}\right)\right\} \qquad (31)$$

If the post is located at the center (D=a/2), then

$$X_o = \frac{k}{4}\left\{-\frac{a}{\pi}\log\left(\frac{2\pi r}{a}\right) + \sum_{\substack{m=2\\ \text{even}}}^{\infty} 2\left(\frac{1}{\gamma_m}-\frac{a}{m\pi}\right)\right\} \qquad (32)$$

These impedances are normalized values with respect to the characteristic impedance of the parallel-plate waveguide. The total post impedance, Z_p, is the sum of the ac IMPATT impedance and this post reactance.

RESULTS

Once the value of the loaded impedance Z_p is known, the characteristics of this structure can be found using the theory of periodic structures. However, a different approach is used here. In practice, it is not necessary to have many diodes and it is also desirable to keep the total line length short to ensure operation at one frequency. That is, the separation of the resonant frequencies becomes large as the length decreases. As Fig. 12 shows, simple admittance transforms are used to analyze the resulting structure. For example,

$$\bar{Y}_1 = \frac{\bar{Y}_L + \tanh \gamma d_{out}}{1 + \bar{Y}_L \tanh \gamma d_{out}} + \bar{Y}_p$$

$$\vdots$$

$$\bar{Y}_{in} = \frac{\bar{Y}_n + \tanh \gamma d_{in}}{1 + \bar{Y}_n \tanh \gamma d_{in}} \qquad (33)$$

The device should oscillate at the frequency where the imaginary part of the input admittance Y_{in} becomes zero.

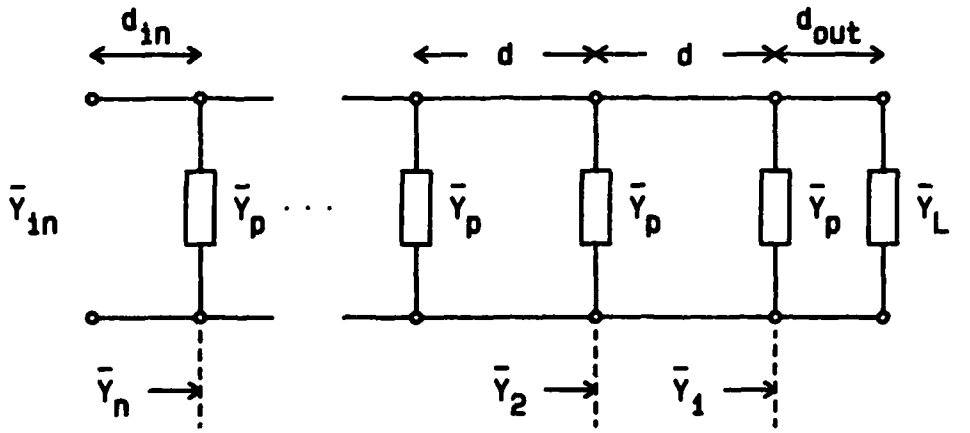

Figure 12 Transmission-line model of the finite-length periodic IMPATT oscillator

As an example, a parallel-plate waveguide loaded with four IMPATT diodes is chosen. Its dimensions and the IMPATT parameters are shown in Table 4. The waveguide is filled with polyimide which has a dielectric constant of ε_r=3.4, and the device ends are assumed to be open-circuited. The calculated input admittance is shown in Fig. 13. Oscillation occurs at 50 GHz in the figure where the imaginary part of Y_{in} becomes zero and the real part negative maximum.

Table 4 Parameters of periodic IMPATT oscillator

length of parallel-plate waveguide	50 mils
width of parallel-plate waveguide	10 mils
distance between diodes	10 mils
IMPATT parameters	
p+ GaAs layer ($N_D=5.0\times10^{24}/m^3$)	0.1 μm
p GaAs layer ($N_D=1.5\times10^{23}/m^3$)	0.35 μm
n GaAs layer ($N_A=1.5\times10^{23}/m^3$)	0.35 μm
n+ GaAs layer ($N_A=5.0\times10^{24}/m^3$)	0.1 μm

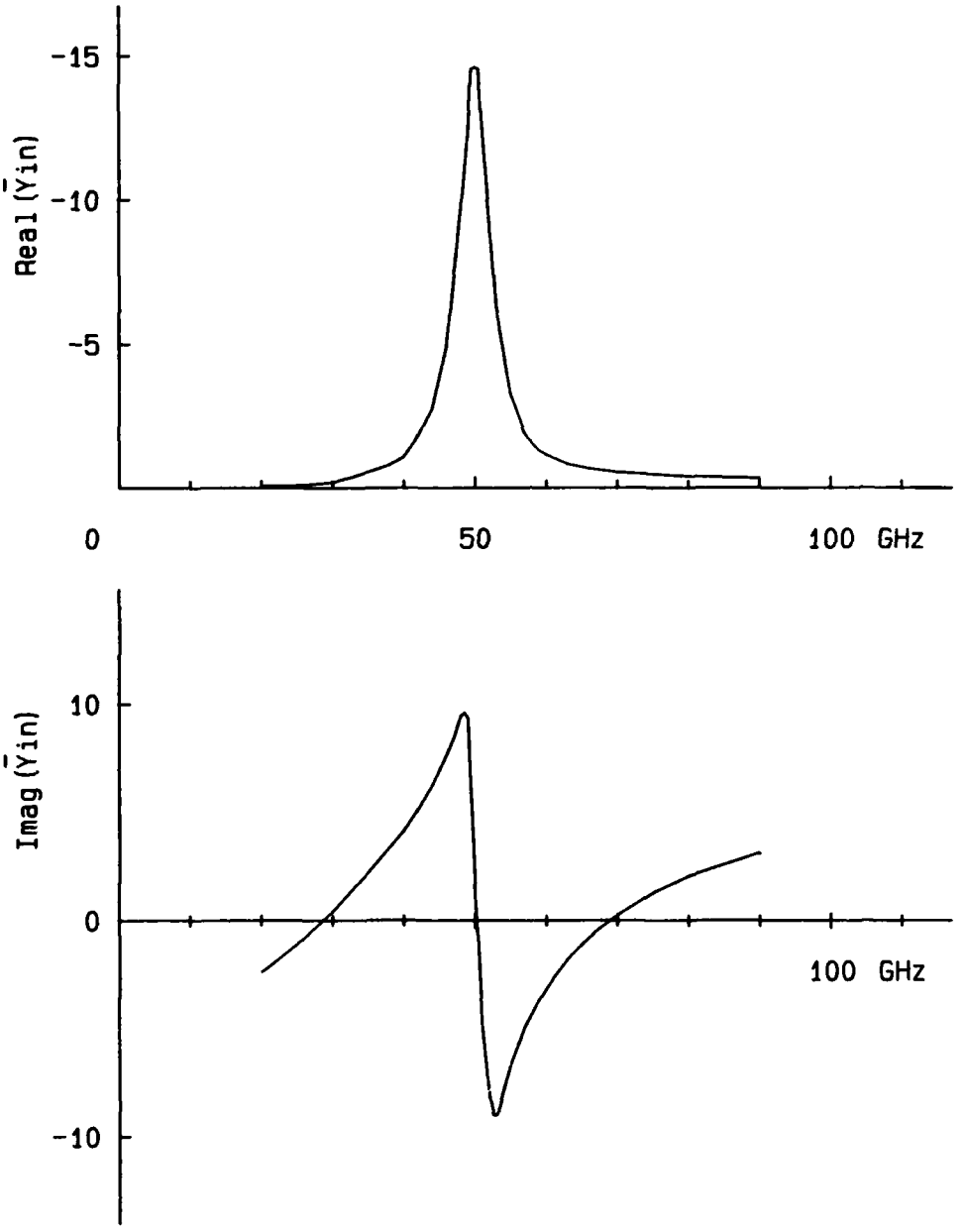

Figure 13 Computed input admittance of the periodic IMPATT oscillator : Resonant frequency is about 50 GHz.

CHAPTER 6 : CONCLUSIONS

Part II covered the theoretical discussion of the travelling-wave IMPATT diode. Small-signal theory governing the behavior of an electromagnetic wave travelling in such a structure was developed. The theory showed the conditions where the device produces gain. Using the theory, one can predict the performance of the travelling-wave IMPATT diode. Experimental results obtained elsewhere confirm the theory, although the device behavior near avalanche resonance could not be predicted well.

The periodic IMPATT oscillator was also discussed as another form of the travelling-wave structure. A simple theory predicted the oscillation frequency.

APPENDIX A : PROGRAM LISTING

Appendix A contains the FORTRAN program code for the analysis of the propagation characteristics of the travelling-wave double-drift IMPATT diode. The subprogram RKF45 is found in the NATEXT library, and ZSPOW and ZANLYT are found in the IMSL library in The University of Texas Numerical Analysis Library.

```
      PROGRAM IMPATT (TTY, OUTPUT, TAPE1, TAPE5=TTY, TAPE6=TTY)
C
C
C
C        COMPUTATION OF THE COMPLEX PROPAGATION CONSTANT
C        OF THE TRAVELLING-WAVE DOUBLE-DRIFT IMPATT DIODE
C
C
C
C        STRUCTURE :
C
C        THE CROSS SECTION OF THE STRUCTURE IS SHOWN
C        BELOW:
C
C                    GOLD
C           ----------------------
C        T1         TITANIUM
C           ----------------------
C        T2         N+ GAAS
C           ----------------------
C        TN         N  GAAS
C           ----------------------
C        TP         P  GAAS
C           ----------------------
C        T3         P+ GAAS
C           ----------------------
C        T4         TITANIUM
C           ----------------------
C                    GOLD
C
C
C        T1 - T4 ... THICKNESS OF EACH LAYER
C                (VALUES ARE ASSIGNED IN THE PROGRAM.)
C        IMPURITY DENSITY OF EACH LAYER IS GIVEN BY
C        THE FUNCTION DENS(X).
C        GOLD LAYERS ARE ASSUMED TO BE SEMI-INFINITELY
C        THICK.
C
C
C        LIBRARIES : NALIB4 (RKF45)
C                    IMSLIBF (ZSPOW, ZANLYT)
C
C
      COMMON       /BASE/PI, DCJ, Q, EPSO, AMUO, OMEGA
      COMMON       /BASEM/VP, VN, GMUN, GMUP, EPSG
      COMMON       /ACTIVE/TN, TP
      COMMON       /BOUND/XI, XF
      COMMON       /LAYER/ZEPSO, ZEPS, T
      COMMON       /PROP/ZGAM, ZD
      COMMON       /ACEXI/ZEXI
      COMPLEX      ZEPSO, ZEPS
      COMPLEX      ZJ, ZGAM, ZEXI, ZD, ZDET, CX
      DIMENSION    ZEPS(6), CX(2), INFER(2)
      DIMENSION    X(2), F(2), PAR(2), WORK(21), S(6), T(6)
      EXTERNAL     FCN1, ZDET
C
C        BASIC CONSTANTS.
C
      ZJ = (0.0, 1.0)
      PI = 3.14159265359
      DBN = 8.6859E-3
```

```
      GMUN = 0.85
      GMUP = 0.04
      G = 1.602E-19
      EPSO = 8.854E-12
      EPSG = 13.0
      AMUO = 4.0*PI/1.E7
      VP = 6.0E4
      VN = 6.0E4
C
C        THICKNESS OF EACH LAYER.
C
      T1 = 0.1E-6
      T2 = 0.2E-6
      T3 = 0.2E-6
      T4 = 0.1E-6
      TN = 0.3E-6
      TP = 0.3E-6
C
C        CONDUCTIVITIES.
C
      SGOLD = 4.3E7
      S(1) = 1.8E6
      S(2) = G*GMUN*DENS(-TN/2.0)
      S(3) = G*GMUN*DENS(TN/2.0)
      S(4) = -G*GMUP*DENS(TN+TP/2.0)
      S(5) = -G*GMUP*DENS(TN+TP+TP/2.0)
      S(6) = 1.8E6
C
C        START DC CALCULATION WHICH DETERMINES
C        THE BOUNDARIES OF THE ACTIVE REGION.
C
 1000 WRITE (6,100)
  100 FORMAT ( /5X,'DC CURRENT (A/M2)' )
      READ (5, * )  DCJ
C
      NSIG = 8
      N = 2
      ITMAX = 50
      X(1) = 0.05*TN
      X(2) = 0.95*(TN+TP)
C
      CALL ZSPOW (FCN1,NSIG,N,ITMAX,PAR,X,FNORM,
     1            WORK,IER)
C
      XI = X(1)
      XF = X(2)
      WRITE (6,200) XI,XF,IER
  200 FORMAT ( /5X,'XI=',E12.6,3X,'XF=',E12.6,3X,'IER=',I3 )
C
C        DETERMINE BOUNDARIES FOR THE CALCULATION
C        OF THE PROPAGATION CONSTANT.
C
      T(1) = T1
      T(2) = T2
      T(3) = XI
      IF ( XI .GE. 0.0 )  GO TO 10
      T(2) = T2+XI
      T(3) = 0.0
   10 T(4) = TN+TP-XF
      T(5) = T3
      IF ( XF  LT  TN+TP )  GO TO 20
      T(4) = 0.0
```

```
      T(5) = T3+TN+TP-XF
   20 T(6) = T4
C
C        START AC CALCULATION WHICH DETERMINES
C        THE COMPLEX PROPAGATION CONSTANT.
C
 2000 WRITE (6,110)
  110 FORMAT ( /5X,'FREQUENCY (GHZ)' )
      READ (5, * )  FREQ
C
      OMEGA = 2.0E9*PI*FREQ
      AKO = OMEGA/3.0E8
      ZEPSO = EPSO-ZJ*SGOLD/OMEGA
      ZEPS(1) = EPSO-ZJ*S(1)/OMEGA
      ZEPS(2) = EPSO*EPSG-ZJ*S(2)/OMEGA
      ZEPS(3) = EPSO*EPSG-ZJ*S(3)/OMEGA
      ZEPS(4) = EPSO*EPSG-ZJ*S(4)/OMEGA
      ZEPS(5) = EPSO*EPSG-ZJ*S(5)/OMEGA
      ZEPS(6) = EPSO-ZJ*S(6)/OMEGA
C
      NSIG = 3
      ITMAX = 25
   30 WRITE (6,230)
  230 FORMAT ( /5X,'INITIAL GUESS : ALPHA, BETA, 1/2'
     1 /21X,'1 ... NEPER/M, /M'
     2 /21X,'2 ... DB/MM, BETA/KO' )
      READ (5, * )  ALPHA1,BETA1,KK
      IF ( KK .EQ. 1 )  GO TO 40
      IF ( KK .NE. 2 )  GO TO 30
      ALPHA1 = ALPHA1/DBN
      BETA1 = BETA1*AKO
   40 CX(1) = ALPHA1 + ZJ*BETA1
      ZEXI = (1.0,1.0)
C
      CALL ZANLYT (ZDET,0.0,NSIG,0,1,1,CX,ITMAX,
     1             INFER,IER)
C
      IF ( AIMAG(CX(1)) .LT. 0.0 )  CX(1) = -CX(1)
      ALPHA1 = REAL(CX(1))
      BETA1 = AIMAG(CX(1))
C
      ALPHA2 = ALPHA1*DBN
      BETA2 = BETA1/AKO
C
      WRITE (6,240)  DCJ,XI,XF,FREQ,
     1               ALPHA1,ALPHA2,BETA1,BETA2,IER
  240 FORMAT ( //5X,'DC CURRENT  = ',E10.4,' A/M'
     1 /8X,'( XI = ',E10.4,',  XF = ',E10.4,' )'
     2 /5X,'FREQUENCY  = ',F6.2,' GHZ'
     3 //5X,'ATTEN. CONST. = ',E10.4,' NEPER/M, ',
     4 E10.4,' DB/MM'/5X,'PROP. CONST.  = ',E10.4,
     5 ' /M, BETA/KO =',F10.6,5X,'IER =',I3 )
      WRITE (1,240)  DCJ,XI,XF,FREQ,
     1               ALPHA1,ALPHA2,BETA1,BETA2,IER
C
   50 WRITE (6,250)
  250 FORMAT ( /5X,'1  ...  CHANGE DC CURRENT'
     1 /5X,'2  ...  CHANGE FREQUENCY'
     2 /5X,'3  ...  CALCULATE FIELD COMPONENTS'
     3 /5X,'4  ...  STOP' )
      READ (5, * )  ICTRL
      IF ( ICTRL .EQ. 1 )  GO TO 1000
```

```
      IF ( ICTRL .EQ. 2 )  GO TO 2000
      IF ( ICTRL .NE. 3 )  STOP
C
      CALL FLDPRT (50)
C
      GO TO 50
C
      END
C
C
C
C
C
      SUBROUTINE FCN1 (X,F,N,PAR)
C
C        SOLVE DC EQUATIONS.
C
      DIMENSION   X(2),F(2),PAR(2),Y(2),WORK(63),IWORK(5)
      COMMON      /RKJUNK/WORK,IWORK
      COMMON      /BASE/PI,DCJ,Q,EPSO,AMUO,OMEGA
      COMMON      /BASEM/VP,VN,GMUN,GMUP,EPSG
      EXTERNAL    DCEQN
C
      NEQN = 2
      IFLAG = 1
      RELERR = 1.0E-8
      ABSERR = 0.0
C
      X1 = X(1)
      X2 = X(2)
      Y(1) = 0.0
      Y(2) = DCJ
C
      CALL RKF45 (DCEQN,NEQN,Y,X1,X2,RELERR,ABSERR,
     1            IFLAG,WORK,IWORK)
C
      IF ( IFLAG .NE. 2 )  GO TO 1000
      F(1) = Y(1)
      F(2) = Y(2)
      WRITE (6,200)  X(1),X(2),F(1),F(2)
  200 FORMAT ( 5X,'XI=',E9.3,' XF=',E9.3,' DCEX=',
     1 E9.3,' DCJN=',E9.3 )
      RETURN
C
 1000 WRITE (6,1010)  IFLAG
 1010 FORMAT ( /5X,'ERROR (FCN1-RKF45) ...  IFLAG=',I3 )
      RETURN
      END
C
C
C
C
C
      SUBROUTINE DCEQN(X,Y,YPRIME)
C
C        DC EQUATIONS.
C
      DIMENSION   Y(2),YPRIME(2)
      COMMON      /BASE/PI,DCJ,Q,EPSO,AMUO,OMEGA
      COMMON      /BASEM/VP,VN,GMUN,GMUP,EPSG
C
      DCEX = Y(1)
```

```
      DCJN = Y(2)
C
      YPRIME(1) = (G*DENS(X)+DCJ/VP-DCJN*(1./VP+1./VN))
     1            /EPSO/EPSG
      YPRIME(2) = -GENA(DCEX)*DCJN-GENB(DCEX)*(DCJ-DCJN)
C
      RETURN
      END
C
C
C
C
C
      COMPLEX FUNCTION ZDET (ZGAMMA)
C
C        SOLVE FOR THE PROPAGATION CONSTANT.
C
      COMPLEX      ZGAMMA, ZGAM, ZEXI, ZD, ZJ
      COMMON       /PROP/ZGAM, ZD
      COMMON       /ACEXI/ZEXI
      EXTERNAL     FCN2
C
      ZGAM = ZGAMMA
      EPS = 0.0
      NSIG = 5
      ITMAX = 25
C
      CALL ZCOMP (FCN2, ZEXI, EPS, NSIG, ITMAX, ICOND)
C
      ZDET = ZD
      WRITE (6,200)  ZGAM, ZDET, ICOND
  200 FORMAT ( 5X, 'ZGAM =', E9.3, X, E9.3, '  ZDET =',
     1 E9.3, X, E9.3, '  ICOND=', I1 )
      RETURN
      END
C
C
C
C
C
      SUBROUTINE FCN2 (ZJN, ZEXI)
C
C        MATCH BOUNDARY CONDITIONS.
C
      DIMENSION    Y(10), WORK(63), IWORK(5)
      DIMENSION    T(6), ZEPS(6)
      COMPLEX      ZEPSO, ZEPS, ZGAM, ZEXI, ZD, ZKX, ZJ
      COMPLEX      ZJP, ZJN, ZEX, ZEXP, ZHY, ZEZ, ZZ1, ZZ2, ZA, ZB
      COMMON       /BASE/PI, DCJ, Q, EPSO, AMUO, OMEGA
      COMMON       /BASEM/VP, VN, GMUN, GMUP, EPSG
      COMMON       /RKJUNK/WORK, IWORK
      COMMON       /BOUND/XI, XF
      COMMON       /PROP/ZGAM, ZD
      COMMON       /LAYER/ZEPSO, ZEPS, T
      EXTERNAL     ACEGN
C
      ZJ = (0.0,1.0)
      ZEX = ZEXI
C
C        UPPER GOLD REGION
C
      ZKX = CSQRT(ZGAM*ZGAM+OMEGA*OMEGA*ZEPSO*AMUO)
```

```
      IF ( AIMAG(ZKX) .GT. 0.0 )  ZKX = -ZKX
      ZHY = (1.0,0.0)
      ZEZ = ZKX/OMEGA/ZEPS0
C
C        TITANIUM, N+ AND N REGIONS
C
      DO 30 I=1,3
      IF ( T(I) .EQ. 0.0 )  GO TO 30
      ZKX = CSQRT(ZGAM*ZGAM+OMEGA*OMEGA*ZEPS(I)*AMU0)
      ZA = 0.5*(ZHY+OMEGA*ZEPS(I)*ZEZ/ZKX)
      ZB = 0.5*(ZHY-OMEGA*ZEPS(I)*ZEZ/ZKX)
      ZHY = ZA*CEXP(ZJ*ZKX*T(I)) + ZB*CEXP(-ZJ*ZKX*T(I))
      ZEZ = (ZA*CEXP(ZJ*ZKX*T(I)) - ZB*CEXP(-ZJ*ZKX*T(I)))
     1     *ZKX/OMEGA/ZEPS(I)
   30 CONTINUE
C
C        ACTIVE REGION
C
      NEQN = 10
      IFLAG = 1
      RELERR = 1.0E-8
      ABSERR = 1.0E-12
      X1 = XI
      X2 = XF
      ZJN = ZGAM*ZHY-ZJ*OMEGA*EPS0*EPSG*ZEX
      ZEXP = ZGAM*ZEZ-ZJN/VN/EPS0/EPSG
      Y(1) = 0.0
      Y(2) = DCJ
      Y(3) = 0.0
      Y(4) = 0.0
      Y(5) = REAL(ZJN)
      Y(6) = AIMAG(ZJN)
      Y(7) = REAL(ZEX)
      Y(8) = AIMAG(ZEX)
      Y(9) = REAL(ZEXP)
      Y(10) = AIMAG(ZEXP)
C
      CALL RKF45 (ACEQN, NEQN, Y, X1, X2, RELERR, ABSERR,
     1            IFLAG, WORK, IWORK)
C
      IF ( IFLAG .NE. 2 )  GO TO 1000
      ZJP = Y(3) + ZJ*Y(4)
      ZJN = Y(5) + ZJ*Y(6)
      ZEX = Y(7) + ZJ*Y(8)
      ZEXP = Y(9) + ZJ*Y(10)
      ZEZ = (ZEXP-(ZJP/VP-ZJN/VN)/EPS0/EPSG)/ZGAM
      ZHY = (ZJ*OMEGA*EPS0*EPSG*ZEX+ZJP+ZJN)/ZGAM
      ZZ1 = ZEZ / ZHY
C
C        LOWER GOLD REGION
C
      ZKX = CSQRT(ZGAM*ZGAM+OMEGA*OMEGA*ZEPS0*AMU0)
      IF ( AIMAG(ZKX) .LT. 0.0 )  ZKX = -ZKX
      ZHY = (1.0,0.0)
      ZEZ = ZKX/OMEGA/ZEPS0
C
C        TITANIUM, P+ AND P REGIONS
C
      DO 40 IDUM=1,3
      I = 7-IDUM
      IF ( T(I) .EQ. 0.0 )  GO TO 40
      ZKX = CSQRT(ZGAM*ZGAM+OMEGA*OMEGA*ZEPS(I)*AMU0)
```

```
      ZA = 0.5*(ZHY+OMEGA*ZEPS(I)*ZEZ/ZKX)
      ZB = 0.5*(ZHY-OMEGA*ZEPS(I)*ZEZ/ZKX)
      ZHY = ZA*CEXP(-ZJ*ZKX*T(I)) + ZB*CEXP(ZJ*ZKX*T(I))
      ZEZ = (ZA*CEXP(-ZJ*ZKX*T(I)) - ZB*CEXP(ZJ*ZKX*T(I)))
     1     *ZKX/OMEGA/ZEPS(I)
   40 CONTINUE
C
      ZZ2 = ZEZ / ZHY
      ZD = ZZ1 - ZZ2
C     WRITE (6,200)  ZEXI,ZJN
C 200 FORMAT ( 5X,'ZEXI=',E9.3,X,E9.3,'  ZJN=',E9.3,
C    1 X,E9.3 )
      RETURN
C
 1000 WRITE (6,1010)  IFLAG
 1010 FORMAT ( /5X,'ERROR (FCN2-RKF45) ...  IFLAG=',I3 )
      RETURN
      END
C
C
C
C
C
      SUBROUTINE ACEQN (X,Y,YPRIME)
C
C        AC EQUATIONS.
C
      DIMENSION    Y(10),YPRIME(10)
      COMPLEX      ZJ,Z1,Z2,Z3,ZJP,ZJN,ZEX,ZEXP
      COMPLEX      ZJPP,ZJNP,ZEXPP,ZGAM,ZD
      COMMON       /BASE/PI,DCJ,Q,EPSO,AMUO,OMEGA
      COMMON       /BASEM/VP,VN,GMUN,GMUP,EPSG
      COMMON       /PROP/ZGAM,ZD
C
      ZJ = (0.0,1.0)
      DCEX = Y(1)
      DCJN = Y(2)
      DCJP = DCJ - DCJN
      ZJP = Y(3) + ZJ*Y(4)
      ZJN = Y(5) + ZJ*Y(6)
      ZEX = Y(7) + ZJ*Y(8)
      ZEXP = Y(9) + ZJ*Y(10)
C
      Z1 = (ZJ*OMEGA+GMUN*DCJN/VN/EPSO/EPSG)/VN - GENA(DCEX)
      Z2 = -GMUN*DCJN/VN/VP/EPSO/EPSG-GENB(DCEX)
      Z3 = -DCJN*GENAP(DCEX)-DCJP*GENBP(DCEX)
      ZJNP = Z1*ZJN+Z2*ZJP+Z3*ZEX+GMUN*DCJN/VN*ZEXP
C
      Z1 = -(ZJ*OMEGA+GMUP*DCJP/VP/EPSO/EPSG)/VP + GENB(DCEX)
      Z2 = GMUP*DCJP/VP/VN/EPSO/EPSG+GENA(DCEX)
      Z3 = DCJN*GENAP(DCEX)+DCJP*GENBP(DCEX)
      ZJPP = Z1*ZJP+Z2*ZJN+Z3*ZEX+GMUP*DCJP/VP*ZEXP
C
      Z1 = -ZGAM*ZGAM-OMEGA*OMEGA*AMUO*EPSO*EPSG
      Z2 = (ZJPP/VP-ZJNP/VN)/EPSO/EPSG
      Z3 = ZJ*OMEGA*AMUO*(ZJN+ZJP)
      ZEXPP = Z1*ZEX + Z2 + Z3
C
     YPRIME(1) = (Q*DENS(X)+DCJP/VP-DCJN/VN)
     1            /EPSO/EPSG
     YPRIME(2) = -GENA(DCEX)*DCJN-GENB(DCEX)*DCJP
     YPRIME(3) = REAL(ZJPP)
```

```
      YPRIME(4) = AIMAG(ZJPP)
      YPRIME(5) = REAL(ZJNP)
      YPRIME(6) = AIMAG(ZJNP)
      YPRIME(7) = REAL(ZEXP)
      YPRIME(8) = AIMAG(ZEXP)
      YPRIME(9) = REAL(ZEXPP)
      YPRIME(10) = AIMAG(ZEXPP)
C
      RETURN
      END
C
C
C
C
C
      SUBROUTINE FLDPRT (M)
C
C        PRINT DC AND AC FIELD COMPONENTS IN
C        THE ACTIVE IMPATT REGION.
C
      DIMENSION    Y(10), WORK(63), IWORK(5)
      DIMENSION    T(6), ZEPS(6)
      COMPLEX      ZJ, ZGAM, ZEXI, ZD, ZEPSO, ZEPS, ZKX
      COMPLEX      ZJP, ZJN, ZEX, ZEXP, ZHY, ZEZ, ZZ1, ZZ2, ZA, ZB
      COMMON       /RKJUNK/WORK, IWORK
      COMMON       /BASE/PI, DCJ, Q, EPSO, AMUO, OMEGA
      COMMON       /BASEM/VP, VN, GMUN, GMUP, EPSG
      COMMON       /BOUND/XI, XF
      COMMON       /LAYER/ZEPSO, ZEPS, T
      COMMON       /PROP/ZGAM, ZD
      COMMON       /ACEXI/ZEXI
      EXTERNAL     ACEQN
C
      ZJ = (0.0,1.0)
      ZEX = ZEXI
C
C        UPPER GOLD REGION
C
      ZKX = CSQRT(ZGAM*ZGAM+OMEGA*OMEGA*ZEPSO*AMUO)
      IF ( AIMAG(ZKX) .GT. 0.0 )  ZKX = -ZKX
      ZHY = (1.0,0.0)
      ZEZ = ZKX/OMEGA/ZEPSO
C
C        TITANIUM, N+ AND N REGIONS
C
      DO 30 I=1,3
      IF ( T(I) .EQ. 0.0 )  GO TO 30
      ZKX = CSQRT(ZGAM*ZGAM+OMEGA*OMEGA*ZEPS(I)*AMUO)
      ZA = 0.5*(ZHY+OMEGA*ZEPS(I)*ZEZ/ZKX)
      ZB = 0.5*(ZHY-OMEGA*ZEPS(I)*ZEZ/ZKX)
      ZHY = ZA*CEXP(ZJ*ZKX*T(I)) + ZB*CEXP(-ZJ*ZKX*T(I))
      ZEZ = (ZA*CEXP(ZJ*ZKX*T(I)) - ZB*CEXP(-ZJ*ZKX*T(I)))
     1    *ZKX/OMEGA/ZEPS(I)
   30 CONTINUE
C
C        ACTIVE REGION
C
      NEQN = 10
      IFLAG = 1
      RELERR = 1.0E-8
      ABSERR = 1.0E-12
      X1 = XI
```

```
      ZJN = ZGAM*ZHY-ZJ*OMEGA*EPSO*EPSG*ZEX
      ZEXP = ZGAM*ZEZ-ZJN/VN/EPSO/EPSG
      Y(1) = 0.0
      Y(2) = DCJ
      Y(3) = 0.0
      Y(4) = 0.0
      Y(5) = REAL(ZJN)
      Y(6) = AIMAG(ZJN)
      Y(7) = REAL(ZEX)
      Y(8) = AIMAG(ZEX)
      Y(9) = REAL(ZEXP)
      Y(10) = AIMAG(ZEXP)
C
      WRITE (1,200)
  200 FORMAT ( //7X,'X',9X,'DCEX',8X,'DCJN',14X,'ACEX',
     1 19X,'ACJP',19X,'ACJN'/ )
      WRITE (6,210)
  210 FORMAT ( /6X,'X',6X,'DCEX',6X,'DCJN',11X,'ACEX',
     1 16X,'ACJP' )
C
      WRITE (1,220)  X1,Y(1),Y(2),Y(7),Y(8),(Y(I),I=3,6)
  220 FORMAT ( 3X,E9.3,2(2X,E10.4),
     1 3(2X,E10.4,X,E10.4) )
      WRITE (6,230)  X1,Y(1),Y(2),Y(7),Y(8),Y(3),Y(4)
  230 FORMAT ( X,E8.2,6(X,E9.3) )
C
      DO 10 J=1,M
      X2 = XI+J*(XF-XI)/M
C
      CALL RKF45 (ACEQN,NEQN,Y,X1,X2,RELERR,ABSERR,
     1            IFLAG,WORK,IWORK)
C
      WRITE (1,220)  X1,Y(1),Y(2),Y(7),Y(8),(Y(I),I=3,6)
      IF ( J.NE.J/10*10 .AND. J.NE.M )  GO TO 10
      WRITE (6,230)  X1,Y(1),Y(2),Y(7),Y(8),Y(3),Y(4)
C
   10 CONTINUE
      RETURN
      END
C
C
C
C
C
      REAL FUNCTION DENS(X)
C
C        IMPURITY DENSITY FUNCTION IN THE
C        IMPATT DIODE.
C
      COMMON       /ACTIVE/TN,TP
C
      IF ( X .GE. 0.0 )  GO TO 10
      DENS = 5.0E24
      RETURN
C
   10 IF ( X .GE. TN )  GO TO 20
      DENS = 1.9E23
      RETURN
C
   20 IF ( X .GE. TN+TP )  GO TO 30
      DENS = -1.5E23
      RETURN
```

```
C
   30 DENS = -5.0E24
      RETURN
      END
C
C
C
C
C
      REAL FUNCTION GENA(DCEX)
C
C        GENERATION RATE FOR ELECTRONS.
C
      IF ( DCEX .LT. 10. )  GO TO 10
      GENA = 3.5E7*EXP(-(6.85E7/DCEX)**2)
      RETURN
   10 GENA = 0.0
      RETURN
      END
C
C
C
C
C
      REAL FUNCTION GENAP(DCEX)
C
C        1ST DERIVATIVE OF GENA(DCEX).
C
      IF ( DCEX .LT. 10. )  GO TO 10
      GENAP = 2.0*(6.85E7)**2*GENA(DCEX)/DCEX**3
      RETURN
   10 GENAP = 0.0
      RETURN
      END
C
C
C
C
C
      REAL FUNCTION GENB(DCEX)
C
C        GENERATION RATE FOR HOLES.
C
      IF ( DCEX .LT. 10. )  GO TO 10
      GENB = 3.5E7*EXP(-(6.85E7/DCEX)**2)
      RETURN
   10 GENB = 0.0
      RETURN
      END
C
C
C
C
C
      REAL FUNCTION GENBP(DCEX)
C
C        1ST DERIVATIVE OF GENB(DCEX).
C
      IF ( DCEX .LT. 10. )  GO TO 10
      GENBP = 2.0*(6.85E7)**2*GENB(DCEX)/DCEX**3
      RETURN
   10 GENBP = 0.0
```

```
      RETURN
      END
C
C
C
C
C
      SUBROUTINE ZCOMP (USER, Z, EPS, NSIG, ITMAX, ICOND )
C
C        COMPLEX ROOT SEARCH : F(Z) = 0.
C
C        USER ...  USER SUPPLIED SUBROUTINE SUBPROGRAM IN
C                  THE FORM USER(F,Z), WHICH RETURNS THE
C                  VALUE OF THE FUNCTION F(Z) CORRESPONDING
C                  TO THE INPUT VALUE OF Z.
C        Z    ...  ON INPUT, Z CONTAINS AN INITIAL GUESS
C                  OF THE ROOT TO BE FOUND.
C        EPS  ...  1ST CONVERGENCE CRITERION.
C                  ABS(Z-ZP) < EPS   :   ZP IS PREVIOUS Z.
C        NSIG ...  2ND CONVERGENCE CRITERION.
C                  ABS((Z-ZP)/Z) < 10**(-NSIG)
C        ITMAX ..  MAXIMUM ALLOWABLE NUMBER OF ITERATION.
C        ICOND ..  ERROR STATUS.
C                  0 = CRITERIA NOT MET (ERROR)
C                  1 = 1ST CRITERION MET
C                  2 = 2ND CRITERION MET
C
      COMPLEX     Z, Z1, Z2, RT, F0, F1, FP, FRT
C
      IT = 1
      DIGT = 10.0**(-NSIG)
      FRT = (0.0,0.0)
C
      Z1 = (1.0,1.0)
      IF ( CABS(Z) .EQ. 0.0 )  GO TO 10
      Z1 = 1.1*Z
   10 RT = Z1
      GO TO 50
   20 IF ( IT .NE. 2 )  GO TO 30
      F1 = FRT
      RT = Z
      GO TO 50
   30 F0 = FRT
      FP = (F1-F0)/(Z1-Z)
      Z2 = Z - F0/FP
      IF ( CABS(Z-Z2) .GE. CABS(Z1-Z2) )  GO TO 40
      Z1 = Z
      F1 = F0
   40 Z = Z2
C
C        CONVERGENCE CHECK
C
      IF ( CABS(Z-Z1) .LT. EPS )  GO TO 60
      IF ( REAL(Z)*AIMAG(Z) .EQ. 0.0 )  GO TO 45
      IF ( ABS(REAL(Z-Z1)/REAL(Z)) .LT. DIGT .AND.
     1     ABS(AIMAG(Z-Z1)/AIMAG(Z)) .LT. DIGT )
     2     GO TO 70
   45 RT = Z
   50 CALL USER(FRT, RT)
      IT = IT + 1
C
C        ITMAX CHECK
```

```
C
      IF ( IT .LE. ITMAX )  GO TO 20
C
C        ITMAX EXCEEDED
C
      WRITE (6,1000)  IT
 1000 FORMAT ( /5X,'ERROR (ZCOMP) ... ITMAX EXCEEDED. (',
     1    I3,')' )
      ICOND = 0
      RETURN
C
   60 ICOND = 1
      RETURN
C
   70 ICOND = 2
      RETURN
      END
C
C
C -- END OF THE PROGRAM --
C
```

REFERENCES

1. T. A. Midford and H. C. Bowers, "A Two-Port IMPATT Diode Travelling Wave Amplifier," Proc. IEEE vol.56, no.10, pp.1724-1725, October 1968.
2. N. S. Davydova, Y. Z. Danyushevskiy, and L. I. Telyatnikov, "Linear Theory of an IMPATT Diode Distributed Microwave Amplifier," Telecommun. and Radio Eng., vol.27, no.8, pp.112-115, August 1972.
3. K. G. Hambleton and P. N. Robson, "Design Considerations for Resonant Travelling Wave IMPATT Oscillators," Int. J. Electronics, vol.35, no.2, pp.225-244, 1973.
4. B. Bayraktaroglu and H. D. Shih, "Integral Packaging for Millimeter-Wave GaAs IMPATT Diodes Prepared by Molecular Beam Epitaxy," Electron. Lett., vol.19, no.9, pp.327-329, April 1983.
5. B. Bayraktaroglu and H. D. Shih, "Millimeter-Wave GaAs Distributed IMPATT Diodes," IEEE Electron Device Lett., vol.EDL-4, no.11, pp.393-395, November 1983.
6. W. T. Read Jr., "A Proposed High-Frequency, Negative-Resistance Diode," Bell Sys. Tech. J., vol.37, no.2, pp.401-446, March 1958.
7. M. Franz and J. B. Beyer, "The Traveling-Wave IMPATT Mode," IEEE Trans. Microwave Theory Tech., vol.MTT-26, no.11, pp.861-865, November 1978.

8. S. M. Sze and G. Gibbons, "Avalanche Breakdown Voltages of Abrupt and Linearly Graded p-n Junctions in Ge, Si, GaAs, and GaP," Applied Physics Lett., vol.8, no.5, pp.111-113, March 1966.

9. G. E. Forsythe, M. A. Malcolm, and C. B. Moler, Computer Methods for Mathematical Computations, New Jersey: Prentice-Hall, 1977.

10. M. Gilden and M. E. Hines, "Electronic Tuning Effects in the Read Microwave Avalanche Diode," IEEE Trans. Electron Devices, vol.ED-13, no.1, p.169-175, January 1966.

11. T. Misawa, "Negative Resistance in p-n Junctions Under Avalanche Breakdown Conditions, Part II," IEEE Trans. Electron Devices, vol.ED-13, no.1, pp.143-151, January 1966.

12. D. L. Scharfetter, W. J. Evans, and R. L. Johnston, "Double-Drift-Region (p+pnn+) Avalanche Diode Oscillators," Proc. IEEE, vol.58, no.7, pp.1131-1133, July 1970.

13. T. E. Seidal and D. L. Scharfetter, "High-Power Millimeter Wave IMPATT Oscillators with Both Hole and Electron Drift Spaces Made by Ion Implantation," Proc. IEEE, vol.58, no.7, pp.1135-1136, July 1970.

14. T. E. Seidel, R. E. Davis, and D. E. Iglesias, "Double-Drift-Region Ion-Implanted Millimeter-Wave IMPATT Diodes," Proc. IEEE, vol.59, no.8, pp.1222-1228, August 1971.

15. B. Bayraktaroglu, Private Communication.

16. L. Lewin, Theory of Waveguides, New York: Halsted Press, 1975.

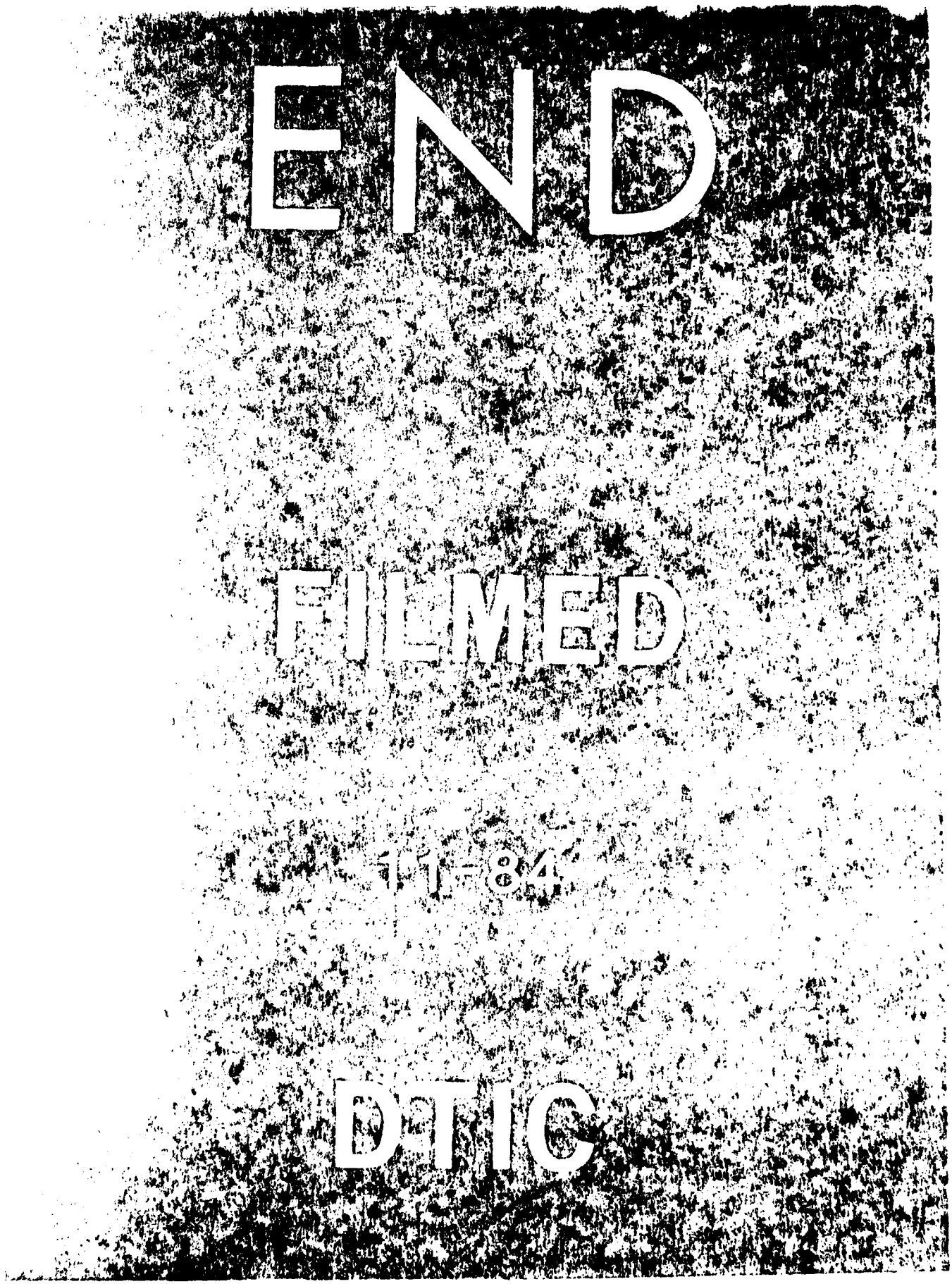
END
FILMED
11-84
DTIC